

Decomposition in Decision and Objective Space for Multi-Modal Multi-Objective Optimization

Monalisa Pal and Sanghamitra Bandyopadhyay*

Abstract

Multi-modal multi-objective optimization problems (MMMOPs) have multiple solution vectors mapping to the same objective vector. For MMMOPs, it is important to discover equivalent solutions associated with each point in the Pareto-Front for allowing end-users to make informed decisions. Prevalent multi-objective evolutionary algorithms are incapable of searching for multiple solution subsets, whereas, algorithms designed for MMMOPs demonstrate degraded performance in the objective space. This motivates the design of better algorithms for addressing MMMOPs. The present work highlights the disadvantage of using crowding distance in the decision space when solving MMMOPs. Subsequently, an evolutionary framework, called graph Laplacian based Optimization using Reference vector assisted Decomposition (LORD), is proposed, which is the first algorithm to use decomposition in both objective and decision space for dealing with MMMOPs. Its filtering step is further extended to present LORD-II algorithm, which demonstrates its dynamics on multi-modal many-objective problems. The efficacy of the frameworks are established by comparing their performance on 34 test instances (obtained from the CEC 2019 multi-modal multi-objective test suite) with the state-of-the-art algorithms for MMMOPs and other multi- and many-objective evolutionary algorithms. The manuscript is concluded mentioning the limitations of the proposed frameworks and future directions to design still better algorithms for MMMOPs.

Keywords: Multi-Modal Multi-Objective Optimization, Non-dominated Sorting, Crowding Distance, Reference vector based Decomposition, Graph Laplacian

*M. Pal and S. Bandyopadhyay are with Machine Intelligence Unit, Indian Statistical Institute, 203 Barrackpore Trunk Road, Kolkata - 700108, West Bengal, India. E-mail: M. Pal (monalisa-pal.r@isical.ac.in) and S. Bandyopadhyay (sanghami@isical.ac.in). This work has been partially supported by Indian Statistical Institute, Kolkata. It has also been supported by J. C. Bose Fellowship (SB/SJ/JCB-033/2016) from Department of Science and Technology, Government of India.

1 Introduction

Multi-objective optimization deals with problems having two or more conflicting objectives (optimization criteria) [1, 2]. The mathematical formulation of a box-constrained multi-objective minimization problem (1) presents the mapping from a N -dimensional vector (\mathbf{X}) in the decision space (\mathcal{D}) to a M -dimensional vector ($\mathbf{F}(\mathbf{X})$) in the objective space [1, 2].

$$\begin{aligned} \text{Minimize } & \mathbf{F}(\mathbf{X}) = [f_1(\mathbf{X}), f_2(\mathbf{X}), \dots, f_M(\mathbf{X})] \\ \text{where, } & \mathbf{X} \in \mathcal{D} (\subseteq \mathbb{R}^N), \mathbf{F}(\mathbf{X}) : \mathcal{D} \mapsto \mathbb{R}^M \\ \text{and } & \mathcal{D} : x_j^L \leq x_j \leq x_j^U, \forall j = 1, 2, \dots, N \end{aligned} \quad (1)$$

Pareto-dominance relation is used for comparison of two vectors i.e., \mathbf{X} Pareto-dominates \mathbf{Y} , as defined below.

$$\begin{aligned} \forall i \in \{1, 2, \dots, M\}, \text{ and } \exists j \in \{1, 2, \dots, M\}, \\ \mathbf{X} \prec \mathbf{Y} \iff (f_i(\mathbf{X}) \leq f_i(\mathbf{Y}) \wedge f_j(\mathbf{X}) < f_j(\mathbf{Y})) \end{aligned} \quad (2)$$

A Pareto-optimal solution $\mathbf{X}^* \in \mathcal{D}$ is attained, if $\nexists \mathbf{X} \in \mathcal{D}$ that dominates \mathbf{X}^* . A set of all such Pareto-optimal solutions form the Pareto-optimal Set (PS) and their images in the objective space yields the Pareto-front (PF) [1, 2].

The notion of Multi-Modal Multi-Objective Problem (MMMOP) [3] arises when a set of k_{PS} (≥ 2) distinct decision vectors ($\mathcal{A}_M = \{\mathbf{X}_1, \mathbf{X}_2, \dots, \mathbf{X}_{k_{PS}}\}$) maps to *almost same* objective vectors i.e., $\forall (\mathbf{X}_i, \mathbf{X}_j) \in \mathcal{A}_M \times \mathcal{A}_M, \|\mathbf{F}(\mathbf{X}_i) - \mathbf{F}(\mathbf{X}_j)\| < \epsilon$ (a small number) as illustrated in Fig. 1 for a benchmark test problem (MMF4 [4]). Thus, the PS can consist of multiple subsets of non-dominated solutions, where each subset can independently generate the entire PF.

The motivation to study MMMOPs arises due to those decision maker's preferences which cannot be mathematically formulated and introduced in the MMMOPs. Thus, providing a diverse set of nearly equivalent solutions help the users to make an informed decision. Another advantage of studying MMMOPs is if the practical implementation of a solution is hindered, an equivalent alternative is readily available. Some practical MMMOPs are seen in rocket engine design [5], feature selection problem [6] and path-planning problem [7].

To optimize such MMMOPs, an Evolutionary Algorithm (EA) faces the following challenges:

1. Maintaining diversity in the decision space i.e., representing and maintaining diversity within each of the multiple solution subsets which independently maps to a diverse approximation of the PF.

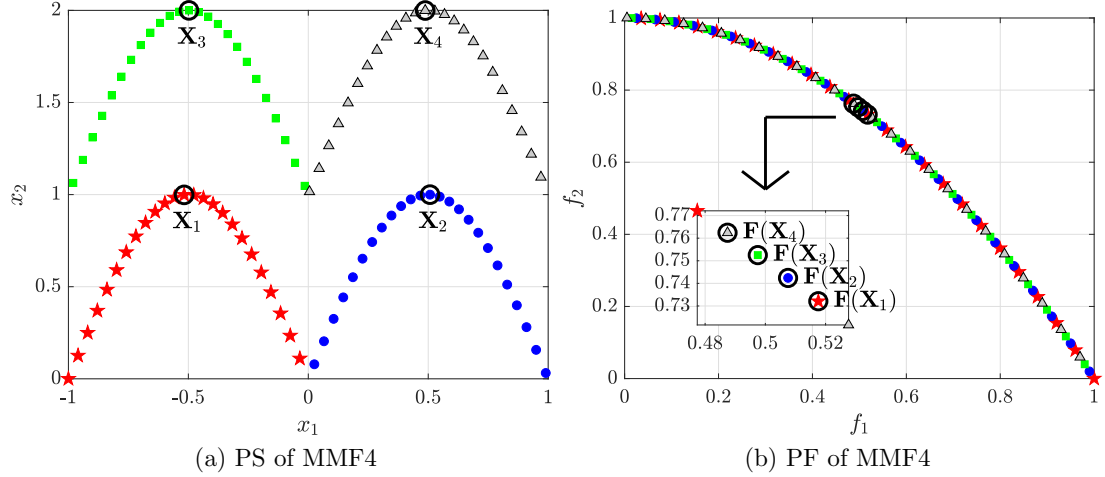


Figure 1: Four solution vectors (\mathbf{X}_1 , \mathbf{X}_2 , \mathbf{X}_3 and \mathbf{X}_4) mapping to *almost same* objective vectors ($\mathbf{F}(\mathbf{X}_1)$, $\mathbf{F}(\mathbf{X}_2)$, $\mathbf{F}(\mathbf{X}_3)$ and $\mathbf{F}(\mathbf{X}_4)$) for a benchmark test problem (MMF4 [4]).

2. Necessity of a large population to efficiently represent an MMMOP. For example, if k_{PF} points (e.g., 100) represent a 2-objective PF and k_{PS} decision vectors (e.g., 4 for MMF4 problem [4, 8]) map to each point of the PF, then the final population size required is $k_{PF} \times k_{PS}$ (e.g., $100 \times 4 = 400$).

Such MMMOPs cannot be tackled by any of the existing Multi-Objective Evolutionary Algorithms (MOEAs) [1, 2]: Pareto-dominance based EAs (such as NSGA-II [9] and θ -DEA [10]), indicator-based EAs (such as HypE [11] and GDE-MOEA [12]) and decomposition-based EAs (such as MOEA/D [13], NSGA-III [14] and MOEA/DD [15]), as these MOEAs focus on the objective space to regulate the population.

For decomposition-based EAs, Das and Dennis's approach [16] is used which involves a two-layered recursive procedure to define reference vectors from the origin to a set of uniformly distributed points on a unit hyperplane in the objective space. These reference vectors partition the objective space into multiple sub-spaces and thereby, reduces the problem complexity by restricting one or more steps of the EA within these subspaces [17]. As these algorithms do not suffer from the dominance resistance phenomenon of Pareto-dominance based EAs [1,2] as well as the huge computational cost of hypervolume-like indicator evaluation [11], decomposition based EAs are extensively used for M -objective problems.

One of the earliest seminal work on assessment and manipulation of solution

distribution in the decision space¹ was that of the Omni-optimizer [18]. It introduced the concept of considering diversity in the decision space during the propagation of *good* candidates. As an indicator of such diversity, it proposed the use of crowding distance in decision space which played a crucial role in the non-dominated sorting strategy. In the direction of incorporating diversity of solutions in both decision as well as objective space, the work in [19] uses neighborhood count and Lebesgue contribution, respectively. However, its evaluation involves large computational cost. Another work [20] which also considered crowding distance in decision space involved a probabilistic model for simultaneously estimating the PSs and the PF. However, it was designed for a special class of problems [20] and has poor performance for problems whose PS is a linear manifold.

Extensive research on EAs for MMMOPs (MMMOEAs) started with decision-niched NSGA-II (DN-NSGA-II) [21] replacing the crowding distance in the objective space with the crowding distance in the decision space in the NSGA-II framework for addressing MMMOPs. Thus, the diversity of solutions in the objective space receives a significant setback. Another study combines NSGA-II with Weighted Sum Crowding Distance and Neighborhood Based Mutation (NSGA-II-WSCD-NBM) [22] for addressing MMMOPs. Unlike these preliminary studies, MO_Ring_PSO_SCD [23] was the first to demonstrate its performance on several MMMOPs. It establishes that both diversity preservation and niching methods (like ring topology) play vital roles for MMMOPs. Zoning search (ZS) [24] was later introduced in MO_Ring_PSO_SCD to enhance its diversity in the decision space. However, as number of zones increases exponentially with the dimension of the decision space, ZS is computationally expensive. After this, MOEA/D with addition and deletion operators (MOEA/D-AD) [25] was proposed which introduced the notion of *almost same* Pareto-optimal solutions, following which Multi-Modal Multi-objective Evolutionary Algorithm with Two Archive and Recombination (TriMOEA_TA&R) strategy [26] was proposed for MMMOPs. Although TriMOEA_TA&R is beneficial only for those MMMOPs where a subspace can be extracted from the convergence-related decision variables [26], it proposed the notion of differential treatment for diversity in decision and in objective space. More specifically, it represented diversity in decision space by neighborhood count. Two recent studies: Differential Evolution based algorithm for MMMOPs (DE-TriM) [8] and Multi-Modal Neighborhood sensitive Archived Evolutionary Multi-Objective optimizer (MM-NAEMO) [27], use reference vector assisted decomposition of objective space and adaptive reproduction strategies for improving diversity in objective space. The former [8] has a performance similar to MO_Ring_PSO_SCD in the decision space but enhanced performance in the objective space whereas the latter [27] has inferior performance in the objective space as compared to other MOEAs. Earlier in 2019, a

¹In this article, decision space, variable space and solution space are considered as synonymous.

Niching Indicator based Multi-Modal Many-Objective optimizer (NIMMO) [28] was proposed which is the first algorithm to demonstrate its performance on a few Multi-Modal Many-Objective Problems (MMMaOPs). However, these MMMaOPs have only 2-dimensional decision space. Overall, most of these algorithms [21, 23, 24, 27] perform poorly in objective space and have been tested only on non-scalable problems which motivate further design of better algorithms to address MMMOPs and MMMaOPs with high number of variables (N) and objectives (M).

The framework proposed in this article is called graph Laplacian based Optimization using Reference vector assisted Decomposition (LORD) and is used for MMMOPs. It is further extended to LORD-II for MMMaOPs. This paper identifies the drawback of using crowding distance in decision space and to reduce its adverse effects, graph Laplacian based clustering (spectral clustering) is used to decompose the decision space while reference vector based approach is used to decompose the objective space. Diversity preservation is conducted in each decomposed sub-region in a collaborative manner. This divide-and-conquer approach uses adaptive hyper-parameters which make the proposed frameworks adaptive to problem characteristics. Analysis of the performance of the proposed frameworks using the test functions from [4] and comparison with other MMMOEAs establish their efficacy.

In the rest of the paper, Section 2 mentions the motivation behind the proposed work, Section 3 outlines the proposed evolutionary frameworks, Section 4 presents the experiments to establish their efficacy and Section 5 concludes the article with scope of future work in this direction.

2 Motivation for the proposed approach

The proposed work is driven by the following motivations:

1. The work in [23] mentions that maintaining good solution distribution is not equivalent to locating more Pareto-optimal solutions. Another work [26] establishes that diversity preservation in decision space is qualitatively represented by the number of optimal solutions and not by their uniform distribution. The reason behind this claim is that the solution distribution is problem-specific. The present work emphasizes both on the number of optimal solutions as well as on their distribution.
2. For MMMOPs, most EAs [8, 18, 20–23] use crowding distance in decision space (CDX) in order to assess the solution distribution. However, the use of crowding distance over the entire decision space can be illusional. To describe the problem, let the example in Fig. 2 be considered. It has an isolated ■ solution in the PS. However, due to overlap along different dimensions of the decision

space, ■ has nearby neighbors in both objective and decision space. Thus, by usual crowding distance based sorting [8, 23], this ■ solution appears towards at the end of the sorted list as a more crowded solution. This problem is being termed as the crowding illusion problem. To reduce the effect of the crowding illusion problem, in this work, a set of non-dominated solutions is clustered and, thereafter, crowding distance is computed within each cluster. By this modified approach, the ■ solution appears towards the beginning of the sorted list as a less crowded solution.

3. The third motivation for presenting the proposed work is to improve the capability of EAs to yield more diverse solutions in the objective space for MMMOPs. To this end, reference vector based decomposition is adopted. Additionally, the proposed approach exploits the neighborhood property [29] during the selection step and attempts to retain solutions if there is only a single solution associated with a direction. Moreover, due to the importance of niching methods for multi-modal optimization, the proposed work uses an adaptive mating among candidates from neighboring directions (subspaces) to generate a progeny.

To the best of the authors' knowledge, the proposed work is the first of its kind to present the concept of decomposition in decision space for handling MMMOPs. Moreover, the proposed framework is also the first to study its scalability on MMaOPs. Herein, lies the novelty of the proposed work.

3 Proposed Algorithmic Framework

This section outlines the overall framework of graph Laplacian based Optimization using Reference vector assisted Decomposition (LORD) while highlighting the major contributions in the population filtering step (line 7 of Algorithm 1).

3.1 General Framework

The overall framework of the proposed algorithm is shown in Algorithm 1. It takes the problem description ($prob(N, M)$) as input along with the population size (n_{pop}), termination condition (maximum function evaluations, $MaxFES$) and the set of reference vectors ($\mathcal{W} = [\mathbf{W}_1, \dots, \mathbf{W}_{n_{dir}}]$) to decompose the objective space. For reference vector assisted decomposition of the objective space, Das and Dennis's approach [16] is used. Algorithm 1 estimates the PS and the PF as the output. Its major blocks are outlined next.

In the initialization phase (line 1), to form the population ($\mathcal{A}_{G=1}$), n_{pop} candidates are randomly generated within the specified bounds of the decision variables

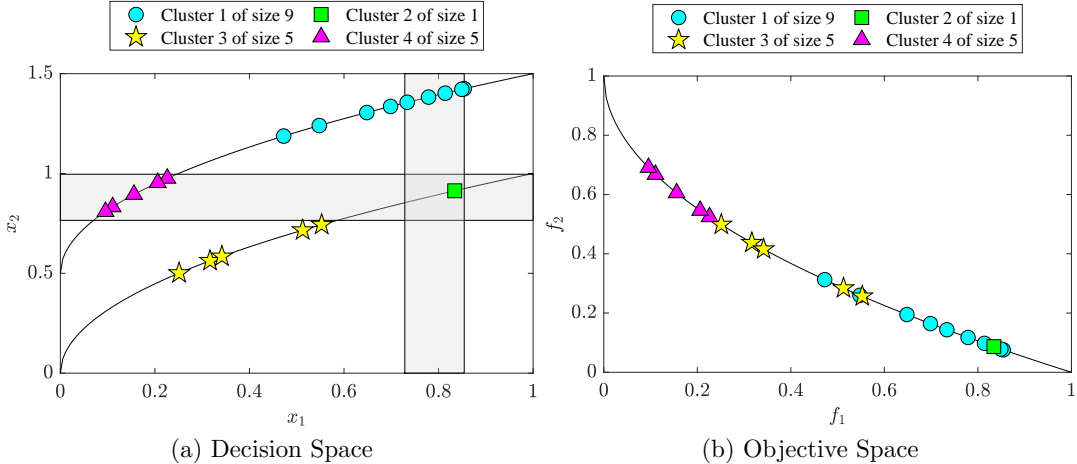


Figure 2: Crowding illusion problem in a benchmark test problem (MMF3 [4]) arises due to overlap along different dimensions of the decision space which gives the illusion that ■ is crowded. Usual sorting of solutions from least crowded to most crowded generates ▲○●★○▲▲★★★★▲○▲○○○○■○ (with ■ solution in 19th position) whereas LORD’s sorting generates ○■★▲○●★▲○★▲○■▲○●○○○ (with ■ solution in 2nd position).

$[\mathbf{X}^L, \mathbf{X}^U]$. Along with this, the mean values of reproduction parameters ($F_{m,G=1}^{DE}$, $CR_{m,G=1}$ and $\eta_{cm,G=1}$) are initialized. For the k^{th} reference vector (\mathbf{W}_k), the indices of other reference vectors are stored in the k^{th} row of the neighborhood lookup matrix, $\mathbf{N}_k \in \mathcal{N}$, sorted by distance from \mathbf{W}_k . This completes the initialization step. The for-loop (line 3 to 13) executes different generations of LORD until $G_{\max} = \lfloor \text{MaxFES}/n_{dir} \rfloor$. Each generation G consists of iterations over all n_{dir} reference vectors. Within one iteration, a number of operations (reproduction/perturbation in line 6 and population filtering in line 7) is performed. These operations are described in the next paragraphs. If the child candidate $\mathbf{X}_{\text{child}}$ survives the filtering step, the reproduction parameters involved in its creation are appended to respective success vectors (\mathbf{S}_{FDE} , \mathbf{S}_{CR} and \mathbf{S}_{η_c}) in steps 8 to 10. When G ends, the mean of reproduction parameters are updated in line 12 over the number of parameter values stored in respective success vectors. The population ($\mathcal{A}_{G_{\max}}$) at the end of G_{\max} generations estimates the PS and the set of objective vectors corresponding to each candidate of $\mathcal{A}_{G_{\max}}$ represents the approximated PF.

The reproduction of a child candidate \mathbf{X}_{child} in line 6 of Algorithm 1 occurs for the k^{th} reference vector (\mathbf{W}_k) by calling Algorithm 2 which is described as follows. The first parent \mathbf{X}_1 is randomly chosen from the candidates associated with \mathbf{W}_k (line

Algorithm 1 General Framework

Input: $prob(N, M)$: An MMMOP having N -dimensional decision space (lower-bounded by \mathbf{X}^L and upper-bounded by \mathbf{X}^U) and M -dimensional objective space; n_{pop} : Population size; $MaxFES$: Maximal of fitness evaluations; \mathcal{W} : Set of n_{dir} reference vectors (as in [15, 16])

Output: $\mathcal{A}_{G_{max}}$: Final population estimating PS; $\mathcal{A}_{\mathbf{F}, G_{max}}$: Objective vectors $\forall \mathbf{X} \in \mathcal{A}_{G_{max}}$ estimating PF

```

1: procedure LORD( $prob, n_{pop}, MaxFES, \mathcal{W}$ )
2:   Set  $\mathcal{A}_G, \mathcal{N}, F_{m,G}^{DE}, CR_{m,G}, \eta_{cm,G}$ , for  $G = 1$ 
3:   for  $G = 1$  to  $G_{max}$  do
4:      $\mathbf{S}_{FDE} \leftarrow \emptyset, \mathbf{S}_{CR} \leftarrow \emptyset, \mathbf{S}_{\eta_c} \leftarrow \emptyset$ 
5:     for  $k = 1$  to  $n_{dir}$  (for each direction) do
6:        $[\mathbf{X}_{child}, F^{DE}, CR, \eta_c] \leftarrow \text{PERTURB}(\mathcal{A}_G,$ 
       $\mathbf{N}_k, F_{m,G}^{DE}, CR_{m,G}, \eta_{cm,G}, \mathbf{W}_k, P_{mut})$ 
7:        $\mathcal{A}_G \leftarrow \text{FILTER}(\mathcal{A}_G, \mathbf{X}_{child})$ 
8:       if  $\mathbf{X}_{child} \in \mathcal{A}_G$  then
9:          $\mathbf{S}_{FDE} \leftarrow \mathbf{S}_{FDE} \cup F^{DE}, \mathbf{S}_{CR} \leftarrow \mathbf{S}_{CR} \cup CR, \mathbf{S}_{\eta_c} \leftarrow \mathbf{S}_{\eta_c} \cup \eta_c$ 
10:      end if
11:      end for
12:       $F_{m,G+1}^{DE} \leftarrow \text{mean}(\mathbf{S}_{FDE}),$ 
       $CR_{m,G+1} \leftarrow \text{mean}(\mathbf{S}_{CR}),$ 
       $\eta_{cm,G+1} \leftarrow \text{mean}(\mathbf{S}_{\eta_c})$ 
13:    end for
14:    return  $\mathcal{A}_{G_{max}}$  and  $\mathcal{A}_{\mathbf{F}, G_{max}} = \{\mathbf{F}(\mathbf{X}) | \mathbf{X} \in \mathcal{A}_{G_{max}}\}$ 
15: end procedure

```

7). The other remaining parents (in line 10 or 17) and also \mathbf{X}_1 if no candidates are associated with \mathbf{W}_k (in lines 3 to 5) are randomly chosen using the same mating pool ($\mathcal{A}_{k,G}^{mat}$) formation principle (Algorithm 3, elaborated in next paragraph). The parameter P_{mut} decides whether to perform DE/rand/1/bin [31,32] or SBX crossover [14,21] (in line 9 or 16). The parameter (η_c) of SBX crossover and the parameters (F^{DE} and CR) of DE/rand/1/bin are sampled from Gaussian distributions with mean values provided by $\eta_{cm,G}$, $F_{m,G}^{DE}$ and $CR_{m,G}$, in lines 11 and 18, respectively. The standard deviation values are empirically chosen. As SBX crossover yields two children, one of them is randomly removed (in line 13). Both SBX crossover and DE/rand/1/bin are followed by Polynomial mutation [30] in lines 14 and 21, respectively. Polynomial mutation [30] helps to avoid local optima and hence, is very effective for MMMOEAs. The child candidate (\mathbf{X}_{child}) and the sampled values of reproduction parameters are returned in line 24. Depending on the choice of if-condition in line 9 of Algorithm 2,

Algorithm 2 Reproduction of Child Candidate

Input: \mathcal{A}_G : Population; \mathbf{N}_k : Mating pool; $\{F_{m,G}^{DE}, CR_{m,G}, \eta_{cm,G}\}$: Reproduction parameters; \mathbf{W}_k : k^{th} reference vector; P_{mut} : Probability of mutation switching

Output: \mathbf{X}_{child} : Child; $\{F^{DE}, CR, \eta_c\}$: Reproduction parameters used

```

1: procedure PERTURB( $\mathcal{A}_G, \mathbf{N}_k, F_{m,G}^{DE}, CR_{m,G}, \eta_{cm,G}, \mathbf{W}_k, P_{mut}$ )
2:   if no candidate is associated with  $\mathbf{W}_k$  then
3:      $\mathbf{N}' \leftarrow$  First  $k_{nbr}$  non-empty vectors from  $\mathbf{N}_k$ 
4:      $\mathbf{W}_r \leftarrow$  Reference vector for random index  $r \in \mathbf{N}'$ 
5:      $\mathbf{X}_1 \leftarrow$  Random candidate associated with  $\mathbf{W}_r$ 
6:   else
7:      $\mathbf{X}_1 \leftarrow$  Random candidate associated with  $\mathbf{W}_k$ 
8:   end if
9:   if  $rand(0, 1) < P_{mut}$  then
10:     $\mathcal{A}_{k,G}^{mat} \leftarrow$  MATING_POOL( $\mathbf{N}_k, \mathcal{A}_G, 1$ )
11:     $\eta_c \leftarrow N(\eta_{cm,G}, 5)$ 
12:     $\mathbf{X}_2 \leftarrow$  Randomly from  $\mathcal{A}_{k,G}^{mat}$ 
13:     $\mathbf{X}'_{child} \leftarrow$  SBX-crossover [14] with  $\mathbf{X}_1, \mathbf{X}_2, \eta_c$ 
14:     $\mathbf{X}_{child} \leftarrow$  Polynomial mutation [30] on  $\mathbf{X}'_{child}$ 
15:     $F^{DE} \leftarrow \emptyset, CR \leftarrow \emptyset$ 
16:  else
17:     $\mathcal{A}_{k,G}^{mat} \leftarrow$  MATING_POOL( $\mathbf{N}_k, \mathcal{A}_G, 3$ )
18:     $F^{DE} \leftarrow N(F_{m,G}^{DE}, 0.1), CR \leftarrow N(CR_{m,G}, 0.1)$ 
19:     $[\mathbf{X}_2, \mathbf{X}_3, \mathbf{X}_4] \leftarrow$  Randomly from  $\mathcal{A}_{k,G}^{mat}$ 
20:     $\mathbf{X}'_{child} \leftarrow$  DE/rand/1/bin [31] with  $\mathbf{X}_1$  to  $\mathbf{X}_4, F^{DE}, CR$ 
21:     $\mathbf{X}_{child} \leftarrow$  Polynomial mutation [30] on  $\mathbf{X}'_{child}$ 
22:     $\eta_c \leftarrow \emptyset$ 
23:  end if
24:  return  $\mathbf{X}_{child}, F^{DE}, CR, \eta_c$ 
25: end procedure

```

either η_c or F^{DE} and CR are empty so only used values of reproduction parameters are appended to the success vectors in line 9 of Algorithm 1.

The mating pool ($\mathcal{A}_{k,G}^{mat}$) formation in line 10 or 17 of Algorithm 2 occurs for the k^{th} reference vector ($\mathbf{W}_k \in \mathcal{W}$) by calling Algorithm 3. The idea is to consider k_{nbr} nearest non-empty reference vectors of \mathbf{W}_k (line 2). Afterwards, n_S random reference vectors $\{\mathbf{W}_{r_1}, \dots, \mathbf{W}_{r_{n_S}}\}$ are selected from these k_{nbr} selected vectors in line 3. All candidates associated with $\{\mathbf{W}_{r_1}, \dots, \mathbf{W}_{r_{n_S}}\}$ form $\mathcal{A}_{k,G}^{mat}$ in line 4 and returned from line 5. For association, the minimum perpendicular distance from the objective vector to a reference vector is considered as done in [14, 15].

Algorithm 3 Mating Pool Formation

Input: \mathbf{N}_k : Sorted array of nearest neighboring directions of \mathbf{W}_k ; \mathcal{A}_G : Population in decision space; n_S : Number of sub-spaces to be chosen

Output: $\mathcal{A}_{k,G}^{mat}$: Sub-population selected for mating

```
1: procedure MATING_POOL( $\mathbf{N}_k$ ,  $\mathcal{A}_G$ ,  $n_S$ )
2:    $\mathbf{N}' \leftarrow$  First  $k_{nbr}$  non-empty vectors from  $\mathbf{N}_k$ 
3:    $\{\mathbf{W}_{r_1}, \dots, \mathbf{W}_{r_{n_S}}\} \leftarrow$  Reference vectors for random indices
    $\{r_1, \dots, r_{n_S}\} \in \mathbf{N}'$ 
4:    $\mathcal{A}_{k,G}^{mat} \leftarrow$  Candidates of  $\mathcal{A}_G$  associated with  $\{\mathbf{W}_{r_1}, \dots, \mathbf{W}_{r_{n_S}}\}$ 
5:   return  $\mathcal{A}_{k,G}^{mat}$ 
6: end procedure
```

In order to maintain the convergence and diversity of the population in the objective space as well as the diversity of the population in the decision space, one of the candidates from the existing population (\mathcal{A}_G) or the child candidate (\mathbf{X}_{child}) is removed in line 7 of Algorithm 1 by calling the filtering operation, which is explained in the next few sub-sections.

3.2 Decomposition of the Decision Space

The selection / filtering step (line 7) of Algorithm 1 involves graph Laplacian based partitioning [33] of the population in the decision space. Let a set of solutions in the decision space be considered as \mathcal{A}^{nd} . The steps for such spectral clustering of \mathcal{A}^{nd} are enumerated as follows:

1) *Create nearest neighbor graph (\mathcal{G}):* All candidates of \mathcal{A}^{nd} are considered as the nodes of graph \mathcal{G} . Euclidean distances between all pairs of candidates in \mathcal{A}^{nd} are evaluated. Edges are placed between pairs of candidates (nodes) where distance is less than a threshold of ε_L . Specifically, \mathcal{G} (binary symmetric matrix) is the adjacency matrix representation.

2) *Obtain symmetric normalized graph Laplacian (\mathcal{L}_{sym}):* The symmetric normalized graph Laplacian [33] is obtained using (3) where I is the identity matrix of the same order as of \mathcal{G} and \mathcal{G}_d is a diagonal matrix created using the degree of each node (row sum) of \mathcal{G} .

$$\mathcal{L}_{sym} = I - \mathcal{G}_d^{-1/2} \mathcal{G} \mathcal{G}_d^{-1/2} \quad (3)$$

3) *Obtain number of connected components (k_{cc}):* The algebraic multiplicity of 0 eigen value of \mathcal{L}_{sym} [33] gives the number of connected components (k_{cc}) of \mathcal{G} .

4) *Assign candidates (nodes) to k_{cc} clusters:* By Cheeger's inequality [34,35], the sparsest cut of a graph is approximated by the second smallest eigenvalue of \mathcal{L}_{sym} .

Algorithm 4 Filter for constant Population Size (LORD)

Input: \mathcal{A}_G : Current population; \mathbf{X}_{child} : Child candidate
Output: \mathcal{A}_G : Filtered population of size n_{pop} ;

```

1: procedure FILTER( $\mathcal{A}_G$ ,  $\mathbf{X}_{child}$ )
2:    $\mathcal{A}_{\mathbf{F},G}^{all} = \{\mathbf{F}(\mathbf{X}) | \mathbf{X} \in (\mathcal{A}_G \cup \mathbf{X}_{child})\}$ 
3:    $\mathcal{A}_{\mathbf{F}}^{nd} \leftarrow$  Last non-dominated rank of  $\mathcal{A}_{\mathbf{F},G}^{all}$ 
4:    $\mathcal{A}^{nd} = \{\mathbf{X} | \mathbf{F}(\mathbf{X}) \in \mathcal{A}_{\mathbf{F}}^{nd}\}$ 
5:    $\{\mathcal{C}_1, \dots, \mathcal{C}_{k_{cc}}\} \leftarrow$  Spectral clustering of  $\mathcal{A}^{nd}$ 
6:   Evaluate SCD cluster-wise
7:    $\mathcal{A}_s^{nd} \leftarrow$  Select one-by-one from  $\mathcal{C}_1$  to  $\mathcal{C}_{k_{cc}}$  w.r.t. SCD
8:   for  $j = |\mathcal{A}_s^{nd}|$  to 1 (starting from most-crowded) do
9:      $\mathbf{W}_k \leftarrow$  Direction where  $\mathbf{X}_j \in \mathcal{A}_s^{nd}$  is associated
10:    if #candidates associated with  $\mathbf{W}_k > 1$  then
11:       $\mathbf{X}_{del} \leftarrow$  Assign  $\mathbf{X}_j$  for deletion
12:      Break loop
13:    end if
14:   end for
15:   if no  $\mathbf{X}_{del}$  is chosen then
16:      $\mathbf{X}_{del} \leftarrow$  Last candidate of  $\mathcal{A}_s^{nd}$ 
17:   end if
18:    $\mathcal{A}_G \leftarrow (\mathcal{A}_G \cup \mathbf{X}_{child}) - \mathbf{X}_{del}$ 
19:   return  $\mathcal{A}_G$ 
20: end procedure

```

Thus, in this work, all the eigen vectors from the second smallest to the k_{CC}^{th} eigenvalues are clustered ($\mathcal{C}_1, \dots, \mathcal{C}_{k_{cc}}$) using k-means algorithm [36] for assigning the candidates of \mathcal{A}^{nd} to the clusters (partitions) in the decision space. Examples of clustering of a non-dominated set of solutions are illustrated in Fig. 2a and Fig. 3a for benchmark test problems [4]: MMF3 and MMF2, respectively.

Although any clustering method can be used to reduce the crowding illusion problem, yet spectral clustering is chosen over k-means clustering on \mathcal{A}^{nd} due to the following reasons: (1) k-means is effective only for globular structures whereas spectral clustering is effective for non-globular structure as well, (2) k_{cc} for k-means is not known apriori whereas k_{cc} for spectral clustering can be obtained mathematically and (3) k-means (performed in the step 4 of spectral clustering of \mathcal{A}^{nd}) becomes independent of the number of decision variables (N).

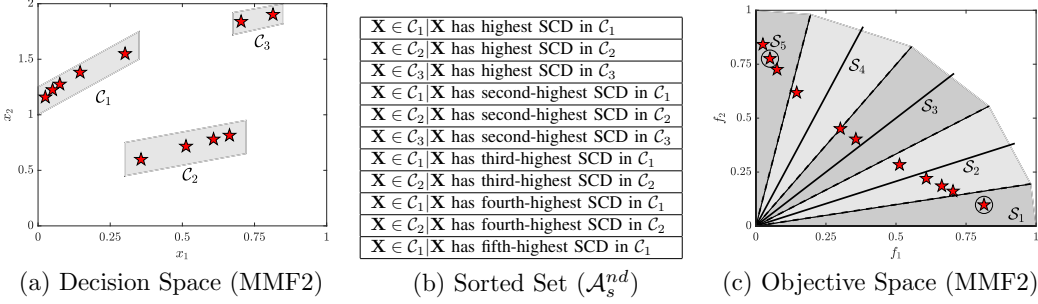


Figure 3: Illustrating the filtering steps of LORD on a non-dominated set of solutions (\mathcal{A}^{nd}) which rearranges candidates by choosing candidates corresponding to maximal SCD from each cluster (\mathcal{C}_1 to $\mathcal{C}_{k_{cc}} = \mathcal{C}_3$) to form the sorted set (\mathcal{A}_s^{nd}). LORD removes one candidate from the end of \mathcal{A}_s^{nd} if it is not the only candidate within a subspace (e.g., the encircled candidate from \mathcal{S}_1 will not be removed, whereas the encircled candidate from \mathcal{S}_5 can be removed).

3.3 Filtering Scheme of LORD framework

The filtering steps of the LORD framework (Algorithm 4) consists of three major steps as follows:

1. *Obtain last non-dominated rank (maintaining convergence in objective space):* The objective vectors corresponding to all candidates of \mathcal{A}_G and \mathbf{X}_{child} are stored in $\mathcal{A}_{\mathbf{F},G}^{all}$ in line 2. Using non-dominated sorting, the subset (\mathcal{A}^{nd}) corresponding to the last non-dominated rank [15, 37] is obtained in lines 3 to 4. If \mathcal{A}^{nd} is a singleton set, lines 5 to 17 yield the only $\mathbf{X}_{del} \in \mathcal{A}^{nd}$ which is eliminated. Otherwise, one of the candidates $\mathbf{X}_{del} \in \mathcal{A}^{nd}$ (i.e., from the least converged set of mutually non-dominated candidates) is to be eliminated.
2. *Spectral clustering of candidates from \mathcal{A}^{nd} (maintaining diversity in decision space):* The candidates in \mathcal{A}^{nd} is partitioned using the steps mentioned in Section 3.2 in line 5. As Special Crowding Distance (SCD) indicates crowding in objective as well as in decision space [8, 23], SCD is evaluated cluster-wise (for all candidates within a cluster) in line 6. A sorted set (\mathcal{A}_s^{nd}) of candidates is formed by rearranging \mathcal{A}^{nd} in line 7 where at first the candidates corresponding to the highest SCD is selected from each cluster, then candidates corresponding to the second-highest SCD is selected from each cluster and so on. Formation of this \mathcal{A}_s^{nd} is shown in Fig. 3b using an example.
3. *Association based elimination of candidate from \mathcal{A}_s^{nd} (maintaining diversity in objective space):* Starting from the last candidate (worst) in \mathcal{A}_s^{nd} , the reference

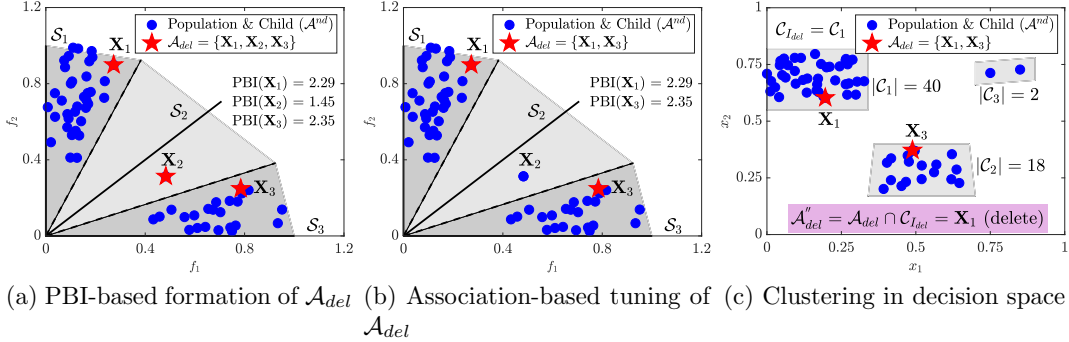


Figure 4: Filtering of LORD-II on a set of solutions (\mathcal{A}^{nd}): (a) candidates (\mathbf{X}_1 , \mathbf{X}_2 and \mathbf{X}_3) with maximal PBI from each sub-space form \mathcal{A}_{del} , (b) sub-spaces with only one candidate (\mathbf{X}_2) are disregarded in \mathcal{A}_{del} , (c) candidate \mathbf{X}_1 , common to both largest cluster ($\mathcal{C}_{I_{del}} = \mathcal{C}_1$ of size 40) and \mathcal{A}_{del} , is deleted.

vector \mathbf{W}_k is obtained in line 9 with which $\mathbf{X}_j \in \mathcal{A}_s^{nd}$ is associated. If multiple candidates of $(\mathcal{A}_G \cup \mathbf{X}_{child})$ are associated with \mathbf{W}_k (showing dense sub-space in objective space), $\mathbf{X}_{del} = \mathbf{X}_j$ is chosen to be deleted (lines 10 to 13). An example is shown in Fig. 3 (please see its caption for further explanation). If all the directions to which candidates of \mathcal{A}_s^{nd} are associated have only one candidate per direction, the last candidate from \mathcal{A}_s^{nd} is chosen to be deleted (lines 15 to 17). The chosen candidate \mathbf{X}_{del} is deleted from $(\mathcal{A}_G \cup \mathbf{X}_{child})$ to yield the filtered population (\mathcal{A}_G) for the next iteration in line 18. This filtered \mathcal{A}_G is returned from line 19 of Algorithm 4 to line 7 of main framework (Algorithm 1).

Explicit maintenance of the three essential properties of an EA for an MMMOP is the most important characteristics of LORD. While SCD explicitly accounts for solution distribution in decision space, the candidates towards the end of \mathcal{A}_s^{nd} come from the largest cluster (as seen in the examples in Fig. 2 and Fig. 3) which are more likely to be deleted. Hence, the proposed framework implicitly takes care of the neighborhood count also as a diversity criterion. This general framework (Algorithm 1) with the filtering scheme in Algorithm 4 is called graph Laplacian based Optimization using Reference vector assisted Decomposition (LORD) whose performance is assessed in Section 4.

3.4 Filtering Scheme of LORD-II framework

As with higher number of objectives, Pareto-dominance fails to provide the necessary selection pressure [1, 2], another filtering scheme using Penalty-based Boundary

Algorithm 5 Filter for constant Population Size (LORD-II)

Input: \mathcal{A}_G : Current population; \mathbf{X}_{child} : Child candidate

Output: \mathcal{A}_G : Filtered population of size n_{pop} ;

```

1: procedure FILTER( $\mathcal{A}_G$ ,  $\mathbf{X}_{child}$ )
2:    $\mathcal{A}^{nd} \leftarrow \mathcal{A}_G \cup \mathbf{X}_{child}$ 
3:    $\mathcal{A}_{\mathbf{F},G}^{nd} = \{\mathbf{F}(\mathbf{X}) | \mathbf{X} \in \mathcal{A}^{nd}\}$ 
4:    $\mathcal{A}_{del} \leftarrow \emptyset$ 
5:   for  $k = 1$  to  $n_{dir}$  (for each direction) do
6:      $\mathcal{A}_{\mathbf{F},k}^{sub} \leftarrow$  Candidates of  $\mathcal{A}_{\mathbf{F},G}^{nd}$  associated with  $\mathbf{W}_k$ 
7:     if  $|\mathcal{A}_{\mathbf{F},k}^{sub}| > 1$  then
8:        $\mathcal{A}_{del} \leftarrow \mathcal{A}_{del} \cup (\mathbf{X} \text{ with max PBI in } \mathcal{A}_{\mathbf{F},k}^{sub})$ 
9:     end if
10:    end for
11:     $[\mathcal{C}_1, \dots, \mathcal{C}_{k_{cc}}] \leftarrow$  Spectral clustering of  $\mathcal{A}^{nd}$ 
12:     $I_{del} = 0, M_{del} = 0$ 
13:    for  $j = 1$  to  $k_{cc}$  (for all clusters) do
14:      if  $\mathcal{A}_{del} \cap \mathcal{C}_j \neq \emptyset$  then
15:        if  $M_{del} < |\mathcal{C}_j|$  then
16:           $I_{del} = j, M_{del} = |\mathcal{C}_j|$ 
17:        end if
18:      end if
19:    end for
20:     $\mathcal{A}_{del}'' \leftarrow \mathcal{C}_{I_{del}} \cap \mathcal{A}_{del}$ 
21:     $\mathbf{X}_{del} \leftarrow$  Select candidate with max PBI from  $\mathcal{A}_{del}''$ 
22:     $\mathcal{A}_G \leftarrow \mathcal{A}^{nd} - \mathbf{X}_{del}$ 
23:    return  $\mathcal{A}_G$ 
24: end procedure

```

Intersection (PBI) is presented in Algorithm 5. The filtering steps of this scheme is illustrated in Fig. 4 which consists of three major steps as follows:

1. *PBI-based selection for deletion (maintaining convergence in objective space):* The objective vectors corresponding to all candidates of \mathcal{A}_G and \mathbf{X}_{child} are stored in $\mathcal{A}_{\mathbf{F},G}^{nd}$ in line 3. From each direction, the candidate with the maximum PBI [15, 16, 38] is stored in \mathcal{A}_{del} (lines 4 to 10) as potential candidates for deletion.
2. *Disregarding based on association (maintaining diversity in objective space):* If the sub-population associated with any direction is a singleton set, its deletion

would hamper the diversity in the objective space. Hence, it is not considered while forming \mathcal{A}_{del} in lines 7 to 10.

3. *Spectral clustering of candidates (maintaining diversity in decision space):* All candidates in decision space (\mathcal{A}^{nd}) is partitioned in line 11 using the steps mentioned in Section 3.2. The density is noted in lines 12 to 19 with respect to cardinality of those clusters which share common element with \mathcal{A}_{del} (line 14). From the largest cluster ($\mathcal{C}_{I_{del}}$), the candidates common to those in \mathcal{A}_{del} are chosen to yield \mathcal{A}_{del}'' in line 20. The candidate with the largest PBI in \mathcal{A}_{del}'' is deleted (lines 21 to 22) to yield the filtered population (\mathcal{A}_G) for the next iteration.

While the cluster size explicitly accounts for the number of optimal solutions in a solution subset, the spectral clustering implicitly accounts for the solution distribution in the decision space. The general framework (Algorithm 1) with this filtering scheme of Algorithm 5 is called LORD-II.

This combination of the proposed operations allows the LORD and LORD-II to effectively address MMMOPs and MMaOPs, respectively, as demonstrated in the next section.

4 Experimental Results

To assess the effectiveness of the proposed frameworks, LORD and LORD-II are implemented in MATLAB R2018a using a 64-bit computer (8 GB RAM, Intel Core i7 @ 2.20 GHz). For performance analysis, the experimental specifications of the benchmark MMMOPs, performance measures, and parameter settings of the proposed as well as competitor algorithms are provided in the following sub-sections.

4.1 Benchmark Problems

The 22 benchmark problems from [4]: MMF1 to MMF15, MMF1_z, MMF1_e, MMF14_a, MMF15_a, Omni-test and SYM-PART (simple and rotated) problems, are considered in this study. As per [4], *MaxFES* and the population size² (n_{pop}) are chosen to be $5000 \times N$ and $100 \times N$, respectively. Further details of these MMMOPS are mentioned in Table 1. Overall, the proposed framework is experimented on 34 test instances. The specifications for the two-layered reference vector based decomposition scheme [14–16, 38] are mentioned in Table 2 with p_1 divisions in the boundary layer and p_2 divisions in the inside layer, yielding n_{dir} number of reference vectors.

²Results by varying n_{pop} and *MaxFES* to match the specifications of NIMMO [28] and MOEA/DD [15] are provided in the supplementary material.

Table 1: Specifications for 2-objective MMMOPs in terms of N -dimensional decision space, upper and lower bounded between \mathbf{X}^U and \mathbf{X}^L having reference point at \mathbf{R}_{HV} for HV calculation with N_{IGD} number of points in the reference set for IGD evaluation and #Sets number of subsets within PS.

Problems	N	\mathbf{X}^L	\mathbf{X}^U	\mathbf{R}_{HV}	N_{IGD}	#Sets
MMF1	2	[1, -1]	[3, 1]	[1.1, 1.1]	400	2
MMF1_z	2	[1, -1]	[3, 1]	[1.1, 1.1]	400	2
MMF1_e	2	[1, -20]	[3, 20]	[1.1, 1.1]	400	2
MMF2	2	[0, 0]	[1, 1]	[1.1, 1.1]	400	2
MMF3	2	[0, 0]	[1, 1.5]	[1.1, 1.1]	400	2
MMF4	2	[-1, 0]	[1, 2]	[1.1, 1.1]	400	4
MMF5	2	[1, -1]	[3, 3]	[1.1, 1.1]	400	4
MMF6	2	[1, -1]	[3, 2]	[1.1, 1.1]	400	4
MMF7	2	[1, -1]	[3, 1]	[1.1, 1.1]	400	2
MMF8	2	[- π , 0]	[\mathpi, 9]	[1.1, 1.1]	400	4
MMF9	2	[0.1, 0.1]	[1.1, 1.1]	[1.21, 11]	400	2
MMF10	2	[0.1, 0.1]	[1.1, 1.1]	[1.21, 13.2]	400	1
MMF11	2	[0.1, 0.1]	[1.1, 1.1]	[1.21, 15.4]	400	1
MMF12	2	[0, 0]	[1, 1]	[1.54, 1.1]	410	1
MMF13	3	[0.1, 0.1, 0.1]	[1.1, 1.1, 1.1]	[1.54, 15.4]	1250	1
MMF14	$M \geq 3$	[0, $\overset{M}{\cdots}, 0]$	[1, $\overset{M}{\cdots}, 1]$	[2.2, $\overset{M}{\cdots}, 2.2]$	1250	2
MMF14_a	$M \geq 3$	[0, $\overset{M}{\cdots}, 0]$	[1, $\overset{M}{\cdots}, 1]$	[2.2, $\overset{M}{\cdots}, 2.2]$	1250	2
MMF15	$M \geq 3$	[0, $\overset{M}{\cdots}, 0]$	[1, $\overset{M}{\cdots}, 1]$	[2.5, $\overset{M}{\cdots}, 2.5]$	1250	1
MMF15_a	$M \geq 3$	[0, $\overset{M}{\cdots}, 0]$	[1, $\overset{M}{\cdots}, 1]$	[2.5, $\overset{M}{\cdots}, 2.5]$	1250	1
Omni-test	3	[0, 0, 0]	[6, 6, 6]	[4.4, 4.4]	600	27
SYM-PART simple	2	[-20, -20]	[20, 20]	[4.4, 4.4]	396	9
SYM-PART rotated	2	[-20, -20]	[20, 20]	[4.4, 4.4]	396	9

The idea is to choose these number of divisions such that $n_{dir} \approx n_{pop} = 100N$. It should be noted that MMF12 has discontinuous PF, hence the number of subsets in the global PS is one per Pareto-optimal patch. Also, for MMF10 to MMF13, MMF15 and MMF15_a, the number of subsets in the global PS is one but these problems have local PSs close to their global PS which make them MMMOPs.

Table 2: Specifications for reference vector based decomposition for problems with M objectives and N decision variables.

M	p_1	p_2	n_{dir}
2	$100N - 1$	0	$100N$
3	23	0	300
5	8	0	495
8	5	2	828
10	4	3	935

4.2 Performance Indicators

Performance of MOEAs are reported in terms of their convergence and diversity abilities in the objective space [1]. Inverted generational distance (IGD) [1, 38] and the hypervolume indicator (HV) [11, 29] are used for MMMOPs with $M = 2$ to assess the performance of the EAs in the objective space. As per [4], the reference points (\mathbf{R}_{HV}) for HV evaluation and the number of points (N_{IGD}) sampled from the true PF and PS to form the reference sets³ for IGD evaluation are specified in Table 1. Convergence metric (CM) [39, 40] with the same reference set as IGD and the D_metric [29, 41] are used for MMMOPs with $M \geq 3$ to respectively assess the individual convergence and diversity performance of the EAs in the objective space.

For performance analysis in decision space, IGD in decision space [20] and Pareto-Set Proximity (PSP) [23] are used for MMMOPs with $M = 2$. In this study, IGDX and IGDF represents IGD values in decision and objective spaces, respectively. For MMMOPs with $M \geq 3$, fraction of non-contributing solutions⁴ in the final population (NSX) [42, 43] and the convergence metric of this non-contributing set (CM_NSX) are noted. In the results, 1/HV (specified as rHV) and 1/PSP (specified as rPSP) are considered such that lower value is the better measure over all the indicators. Brief description of all the performance indicators are provided in Section II of the supplementary material for convenience of the readers.

4.3 Details of Competitor Algorithms

As DN-NSGA-II³ [21] and MO_Ring_PSO_SCD³ [23] are MMMOEAs using non-dominated sorting approach with crowding distance in decision space, the perfor-

³The data for reference sets of PS and PF for IGD evaluation, and the MATLAB codes of DN-NSGA-II and MO_Ring_PSO_SCD are acquired from <http://www5.zzu.edu.cn/ecilab/info/1036/1163.htm>.

⁴A non-contributing solution is a solution in the non-dominated set whose removal does not change the IGDX of the non-dominated set.

mance of the proposed framework of LORD is compared with these two algorithms. However, as these MMMOEAs are known to perform poorly in the objective space [21, 23], in order to establish that the efficacy of LORD in the objective space as well, its performance is compared with the most commonly used MOEA (NSGA-II) [2, 44]. For MMMOPs with $M \geq 3$, the performance of LORD-II is compared with MO_Ring_PSO_SCD [23] and a popular decomposition based many-objective optimization algorithm (MOEA/DD⁵) [15].

Other MMMOEAs such as Omni-Optimizer [18], TriMOEA_TA&R [26], MM-NAEMO [27], DE-TriM [8] and NIMMO [28], have demonstrated their effectiveness only for certain kinds of test problems. In Section IV of the supplementary material, some results (from problems of CEC 2019 test suite [4] and from polygon and rotated polygon problems [28, 45]) obtained by these competing algorithms are also compared with those obtained by LORD and LORD-II. These results also support the superiority of the proposed approaches.

Most of the hyper-parameters of LORD and LORD-II are adaptive in nature, while the rest of them are set as follows:

- k_{nbr} is the number of non-empty neighboring directions considered for choosing the mating pool (line 2, Algorithm 3). In this work, $k_{nbr} = 0.2 \times n_{dir}$ is considered. The performance is unaffected when the 0.2 factor is increased. This is because a non-empty neighboring direction is easily found from 20% of all the reference vectors as most of the test instances have regular Pareto-Fronts.
- P_{mut} is the probability of switching between the two reproduction strategies (line 7, Algorithm 2). In this work, $P_{mut} = 0.25$ is considered.
- ε_L is the threshold for formation of nearest neighbor graph in the decision space (Section 3.2). This work considers $\varepsilon_L = \alpha_L \times$ the diagonal of \mathcal{D} , with $\alpha_L = 0.2$.
- The initial mean values for the reproduction parameters are considered to be $F_{m,G=1}^{DE} = 0.5$, $CR_{m,G=1} = 0.2$ and $\eta_{cm,G=1} = 30$.

Studies on the sensitivity of P_{mut} and α_L are provided in Section III of the supplementary material.

4.4 Performance Analysis

For 2-objective MMMOPs, the performance of LORD in decision and objective spaces are presented in Tables 3 and 4, respectively. For M -objective MMMOPs (with $M \geq 3$), the performance of LORD-II is presented in Table 5.

⁵The MATLAB code for MOEA/DD is acquired from <https://github.com/BIMK/PlatEMO>

Table 3: Mean \pm Standard Deviation (Significance) of rPSP and IGDX for 2-objective MMMOPs over 51 Runs.

Problems	rPSP=IGDX/cov_rate				IGDX			
	LORD	MO_Ring_PSO_SCD	DN-NSGA-II	NSGA-II	LORD	MO_Ring_PSO_SCD	DN-NSGA-II	NSGA-II
MMF1	0.0441 \pm 0.0044	0.0489 \pm 0.0018 (+)	0.0957 \pm 0.0146 (+)	0.0652 \pm 0.0103 (+)	0.0431 \pm 0.0044	0.0485 \pm 0.0017 (+)	0.0939 \pm 0.0141 (+)	0.0645 \pm 0.0098 (+)
MMF1 $_{\mathcal{Z}}$	0.0356 \pm 0.0069	0.0354 \pm 0.0019 (~)	0.0822 \pm 0.0166 (+)	0.3892 \pm 0.3913 (+)	0.0351 \pm 0.0075	0.0352 \pm 0.0018 (~)	0.0805 \pm 0.0157 (+)	0.2606 \pm 0.1608 (+)
MMF1 $_{\text{e}}$	0.8894 \pm 0.1466	0.5501 \pm 0.1276 (-)	1.7201 \pm 1.2086 (+)	14.0870 \pm 8.1289 (+)	0.7499 \pm 0.4192	0.4738 \pm 0.0847 (-)	1.1536 \pm 0.5095 (+)	3.0324 \pm 0.7634 (+)
MMF2	0.0219 \pm 0.0108	0.0444 \pm 0.0113 (+)	0.1356 \pm 0.0805 (+)	0.0766 \pm 0.0402 (+)	0.0180 \pm 0.0093	0.0416 \pm 0.0103 (+)	0.1121 \pm 0.0525 (+)	0.0650 \pm 0.0300 (+)
MMF3	0.0200 \pm 0.0105	0.0294 \pm 0.0074 (+)	0.1249 \pm 0.1291 (+)	0.0785 \pm 0.0416 (+)	0.0176 \pm 0.0080	0.0276 \pm 0.0061 (+)	0.0968 \pm 0.0632 (+)	0.0661 \pm 0.0311 (+)
MMF4	0.0253 \pm 0.0036	0.0274 \pm 0.0014 (+)	0.0854 \pm 0.0232 (+)	0.1066 \pm 0.0468 (+)	0.0251 \pm 0.0039	0.0271 \pm 0.0014 (+)	0.0849 \pm 0.0230 (+)	0.1004 \pm 0.0411 (+)
MMF5	0.0814 \pm 0.0080	0.0864 \pm 0.0045 (+)	0.1788 \pm 0.0179 (+)	0.1525 \pm 0.0296 (+)	0.0814 \pm 0.0074	0.0857 \pm 0.0044 (+)	0.1763 \pm 0.0165 (+)	0.1478 \pm 0.0265 (+)
MMF6	0.0692 \pm 0.0104	0.0741 \pm 0.0044 (+)	0.1453 \pm 0.0176 (+)	0.1410 \pm 0.0272 (+)	0.0692 \pm 0.0104	0.0736 \pm 0.0042 (+)	0.1433 \pm 0.0173 (+)	0.1372 \pm 0.0251 (+)
MMF7	0.0219 \pm 0.0044	0.0264 \pm 0.0014 (+)	0.0535 \pm 0.0098 (+)	0.0452 \pm 0.0132 (+)	0.0218 \pm 0.0025	0.0262 \pm 0.0014 (+)	0.0524 \pm 0.0092 (+)	0.0420 \pm 0.0106 (+)
MMF8	0.0745 \pm 0.0452	0.0679 \pm 0.0049 (~)	0.2969 \pm 0.1120 (+)	0.9348 \pm 0.4682 (+)	0.0762 \pm 0.0504	0.0673 \pm 0.0048 (~)	0.2860 \pm 0.1078 (+)	0.7198 \pm 0.3034 (+)
MMF9	0.0047 \pm 0.0002	0.0079 \pm 0.0005 (+)	0.0229 \pm 0.0081 (+)	1.7445 \pm 1.9877 (+)	0.0046 \pm 0.0002	0.0079 \pm 0.0005 (+)	0.0229 \pm 0.0081 (+)	0.1783 \pm 0.0740 (+)
MMF10	0.0018 \pm 0.0007	0.0293 \pm 0.0113 (+)	0.1426 \pm 0.0834 (~)	0.0398 \pm 0.1184 (~)	0.0018 \pm 0.0009	0.0276 \pm 0.0092 (+)	0.1295 \pm 0.0747 (+)	0.0398 \pm 0.1184 (~)
MMF11	0.0029 \pm 0.0002	0.0055 \pm 0.0003 (+)	0.0045 \pm 0.0003 (+)	0.0027 \pm 0.0003 (-)	0.0029 \pm 0.0002	0.0054 \pm 0.0003 (+)	0.0045 \pm 0.0003 (+)	0.0027 \pm 0.0003 (-)
MMF12	0.0013 \pm 0.0001	0.0038 \pm 0.0003 (+)	0.0090 \pm 0.0159 (+)	0.0013 \pm 0.0002 (~)	0.0013 \pm 0.0001	0.0038 \pm 0.0003 (+)	0.0090 \pm 0.0159 (+)	0.0013 \pm 0.0002 (~)
MMF13	0.0243 \pm 0.0039	0.0317 \pm 0.0014 (+)	0.0614 \pm 0.0070 (+)	0.1492 \pm 0.0652 (+)	0.0242 \pm 0.0039	0.0314 \pm 0.0013 (+)	0.0609 \pm 0.0064 (+)	0.0880 \pm 0.0173 (+)
Omnitest	0.0754 \pm 0.0242	0.3946 \pm 0.0939 (+)	1.4390 \pm 0.2069 (+)	1.8176 \pm 0.6886 (+)	0.0706 \pm 0.0215	0.3907 \pm 0.0927 (+)	1.4159 \pm 0.1986 (+)	1.4210 \pm 0.3726 (+)
SYM-PART simple	0.0556 \pm 0.0145	0.1741 \pm 0.0301 (+)	4.1590 \pm 0.8683 (+)	113.0044 \pm 131.2343 (+)	0.0549 \pm 0.0130	0.1733 \pm 0.0300 (+)	4.0657 \pm 0.7040 (+)	6.8332 \pm 1.8906 (+)
SYM-PART rotated	0.1730 \pm 0.0743	0.3142 \pm 0.3533 (+)	5.5941 \pm 3.6017 (+)	13.9239 \pm 12.8588 (+)	0.1558 \pm 0.0760	0.2926 \pm 0.2938 (+)	3.7659 \pm 1.2478 (+)	5.4249 \pm 1.9790 (+)
Sum-up	+/-/~	15/1/2	18/0/0	15/1/2	+/-/~	15/1/2	18/0/0	15/1/2

All the results have been statistically validated using Wilcoxon ranked sum test for all 34 test cases for establishing the superiority of observed performance values of LORD or LORD-II in comparison to the other competitor EAs. The significance is indicated using the following three signs:

- + denotes LORD or LORD-II is significantly superior
- - denotes the competitor EA is significantly superior than LORD or LORD-II
- ~ denotes that LORD or LORD-II has equivalent performance as that of the competitor EA

The following insights can be obtained from the results presented in Tables 3 and 4:

Table 4: Mean \pm Standard Deviation (Significance) of rHV and IGDF for 2-objective MMMOPs over 51 Runs.

Problems	rHV=1/HV				IGDF			
	LORD	MO_Ring_PSO_SCD	DN-NSGA-II	NSGA-II	LORD	MO_Ring_PSO_SCD	DN-NSGA-II	NSGA-II
MMF1	1.0737 \pm 0.0008	1.1484 \pm 0.0005 (+)	1.1495 \pm 0.0014 (+)	1.0738 \pm 0.0006 (\sim)	0.0025 \pm 0.0002	0.0037 \pm 0.0002 (+)	0.0043 \pm 0.0005 (+)	0.0028 \pm 0.0004 (+)
MMF1 _z	1.0731 \pm 0.0008	1.1483 \pm 0.0005 (+)	1.1484 \pm 0.0009 (+)	1.1255 \pm 0.0615 (+)	0.0022 \pm 0.0001	0.0036 \pm 0.0002 (+)	0.0036 \pm 0.0004 (+)	0.0396 \pm 0.0496 (+)
MMF1 _e	1.0751 \pm 0.0021	1.1861 \pm 0.0173 (+)	1.2080 \pm 0.0387 (+)	1.1058 \pm 0.0180 (+)	0.0029 \pm 0.0006	0.0119 \pm 0.0017 (+)	0.0276 \pm 0.0207 (+)	0.0250 \pm 0.0139 (+)
MMF2	1.0817 \pm 0.0120	1.1848 \pm 0.0059 (+)	1.1944 \pm 0.0322 (+)	1.1168 \pm 0.0280 (+)	0.0070 \pm 0.0031	0.0207 \pm 0.0034 (+)	0.0325 \pm 0.0238 (+)	0.0300 \pm 0.0182 (+)
MMF3	1.0792 \pm 0.0322	1.1739 \pm 0.0043 (+)	1.1873 \pm 0.0398 (+)	1.1089 \pm 0.0212 (+)	0.0069 \pm 0.0023	0.0154 \pm 0.0025 (+)	0.0263 \pm 0.0308 (+)	0.0229 \pm 0.0126 (+)
MMF4	1.5234 \pm 0.0003	1.8620 \pm 0.0021 (+)	1.8577 \pm 0.0012 (+)	1.5241 \pm 0.0004 (+)	0.0018 \pm 0.0002	0.0037 \pm 0.0004 (+)	0.0032 \pm 0.0002 (+)	0.0024 \pm 0.0002 (+)
MMF5	1.0734 \pm 0.0006	1.1485 \pm 0.0006 (+)	1.1488 \pm 0.0015 (+)	1.0739 \pm 0.0003 (+)	0.0024 \pm 0.0001	0.0037 \pm 0.0001 (+)	0.0039 \pm 0.0007 (+)	0.0028 \pm 0.0002 (+)
MMF6	1.0732 \pm 0.0003	1.1483 \pm 0.0009 (+)	1.1486 \pm 0.0016 (+)	1.0738 \pm 0.0006 (+)	0.0023 \pm 0.0001	0.0035 \pm 0.0002 (+)	0.0036 \pm 0.0003 (+)	0.0026 \pm 0.0002 (+)
MMF7	1.0731 \pm 0.0002	1.1484 \pm 0.0009 (+)	1.1498 \pm 0.0011 (+)	1.0736 \pm 0.0003 (+)	0.0022 \pm 0.0001	0.0037 \pm 0.0003 (+)	0.0039 \pm 0.0003 (+)	0.0027 \pm 0.0003 (+)
MMF8	1.7915 \pm 0.0012	2.4065 \pm 0.0164 (+)	2.3813 \pm 0.0025 (+)	1.7920 \pm 0.0014 (\sim)	0.0025 \pm 0.0001	0.0048 \pm 0.0002 (+)	0.0040 \pm 0.0004 (+)	0.0025 \pm 0.0001 (\sim)
MMF9	0.0820 \pm 0.0000	0.1034 \pm 0.0000 (+)	0.1034 \pm 0.0000 (\sim)	0.0820 \pm 0.0000 (\sim)	0.0085 \pm 0.0007	0.0160 \pm 0.0014 (+)	0.0141 \pm 0.0012 (+)	0.0108 \pm 0.0007 (+)
MMF10	0.0678 \pm 0.0000	0.0679 \pm 0.0000 (+)	0.0680 \pm 0.0001 (+)	0.0678 \pm 0.0001 (\sim)	0.0061 \pm 0.0009	0.1128 \pm 0.0230 (+)	0.1446 \pm 0.0660 (+)	0.0074 \pm 0.0000 (+)
MMF11	0.0581 \pm 0.0000	0.0581 \pm 0.0000 (\sim)	0.0581 \pm 0.0000 (\sim)	0.0581 \pm 0.0000 (\sim)	0.0082 \pm 0.0004	0.0176 \pm 0.0018 (+)	0.0136 \pm 0.0014 (+)	0.0107 \pm 0.0008 (+)
MMF12	0.5431 \pm 0.0000	0.5452 \pm 0.0014 (+)	0.5598 \pm 0.0492 (\sim)	0.5430 \pm 0.0000 (-)	0.0020 \pm 0.0001	0.0068 \pm 0.0006 (+)	0.0110 \pm 0.0187 (+)	0.0020 \pm 0.0001 (\sim)
MMF13	0.0444 \pm 0.0000	0.0444 \pm 0.0000 (\sim)	0.0444 \pm 0.0000 (\sim)	0.0444 \pm 0.0000 (\sim)	0.0063 \pm 0.0014	0.0264 \pm 0.0076 (+)	0.0121 \pm 0.0036 (+)	0.0089 \pm 0.0014 (+)
Omnitest	0.0518 \pm 0.0000	0.0190 \pm 0.0000 (-)	0.0189 \pm 0.0000 (-)	0.0518 \pm 0.0000 (\sim)	0.0091 \pm 0.0015	0.0422 \pm 0.0034 (+)	0.0080 \pm 0.0005 (-)	0.0100 \pm 0.0021 (\sim)
SYM-PART simple	0.0520 \pm 0.0000	0.0605 \pm 0.0001 (+)	0.0601 \pm 0.0000 (\sim)	0.0520 \pm 0.0000 (\sim)	0.0165 \pm 0.0039	0.0419 \pm 0.0044 (+)	0.0127 \pm 0.0014 (-)	0.0109 \pm 0.0013 (-)
SYM-PART rotated	0.0520 \pm 0.0000	0.0606 \pm 0.0001 (+)	0.0601 \pm 0.0000 (+)	0.0520 \pm 0.0000 (\sim)	0.0178 \pm 0.0047	0.0467 \pm 0.0058 (+)	0.0152 \pm 0.0022 (-)	0.0159 \pm 0.0040 (-)
Sum-up	+/-/ \sim	15/1/2	14/1/3	8/1/9	+/-/ \sim	18/0/0	15/3/0	13/1/4

- LORD has superior performance than DN-NSGA-II [21] in all cases. The reason for the poor performance of DN-NSGA-II is that it considers crowding distance only in decision space and neglects the diversity of solutions in the objective space, which does not allow solutions to spread along the PF. As a result of this behavior and the neighborhood property [29], the solution distribution in the decision space also suffers.
- NSGA-II performs second-best to LORD in the objective space (Table 4). However, as it does not attend to the solution distribution in the decision space, its performance suffers a setback in the decision space (Table 3).
- MO_Ring_PSO_SCD performs second-best to LORD in the decision space (Table 3). However, MO_Ring_PSO_SCD has a tendency to get trapped in the local PS.

Table 5: Mean \pm Standard Deviation (Significance) of NSX, CM_NSX, D_metric and CM for M -objective ($M \geq 3$) MMMOPs over 51 Runs.

Problems (M)	NSX			CM_NSX			D_metric			CM		
	LORD-II	MO.Ring-PSO_SCD	MOEA/DD	LORD-II	MO.Ring-PSO_SCD	MOEA/DD	LORD-II	MO.Ring-PSO_SCD	MOEA/DD	LORD-II	MO.Ring-PSO_SCD	MOEA/DD
MMF14 (3)	0.0068 \pm 0.0052	0.2400 \pm 0.0262 (+)	0.0133 \pm 0.0024 (+)	0.0203 \pm 0.0018	0.1078 \pm 0.0088 (+)	0.0228 \pm 0.0019 (+)	0.0000 \pm 0.0000	21.3266 \pm 2.0086 (+)	0.0000 \pm 0.0000 (~)	0.0419 \pm 0.0003	0.1083 \pm 0.0130 (+)	0.0419 \pm 0.0002 (~)
MMF14_a (3)	0.0251 \pm 0.0290	0.2533 \pm 0.0320 (+)	0.1333 \pm 0.0259 (+)	0.1498 \pm 0.0518	0.1534 \pm 0.0147 (+)	0.2481 \pm 0.0103 (+)	0.0000 \pm 0.0000	22.2752 \pm 2.2816 (+)	0.0000 \pm 0.0000 (~)	0.0435 \pm 0.0007	0.0949 \pm 0.0149 (+)	0.0438 \pm 0.0010 (~)
MMF15 (3)	0.0205 \pm 0.0073	0.4033 \pm 0.0361 (+)	0.0400 \pm 0.0024 (+)	0.0209 \pm 0.0010	0.2356 \pm 0.0251 (+)	0.0265 \pm 0.0039 (~)	0.0000 \pm 0.0000	24.4073 \pm 3.8341 (+)	0.0000 \pm 0.0000 (~)	0.0422 \pm 0.0004	0.1471 \pm 0.0161 (+)	0.0426 \pm 0.0004 (~)
MMF15_a (3)	0.0179 \pm 0.0076	0.3400 \pm 0.0262 (+)	0.0567 \pm 0.0024 (+)	0.0270 \pm 0.0180	0.2068 \pm 0.0263 (+)	0.0454 \pm 0.0098 (+)	0.0000 \pm 0.0000	22.5315 \pm 3.5845 (+)	0.0000 \pm 0.0000 (~)	0.0445 \pm 0.0007	0.1322 \pm 0.0207 (+)	0.0449 \pm 0.0008 (~)
MMF14 (5)	0.4838 \pm 0.0125	0.5140 \pm 0.0168 (+)	0.5152 \pm 0.0057 (+)	0.1830 \pm 0.0015	0.2363 \pm 0.0047 (+)	0.1874 \pm 0.0015 (+)	0.0000 \pm 0.0000	43.9023 \pm 4.6565 (+)	0.0000 \pm 0.0000 (~)	0.0590 \pm 0.0020	0.4121 \pm 0.0177 (+)	0.0587 \pm 0.0015 (~)
MMF14_a (5)	0.4855 \pm 0.0141	0.4960 \pm 0.0175 (~)	0.5232 \pm 0.0029 (+)	0.2080 \pm 0.0155	0.2808 \pm 0.0041 (+)	0.2474 \pm 0.0044 (+)	0.0000 \pm 0.0000	46.7494 \pm 2.8893 (+)	0.9428 \pm 0.8165 (+)	0.0781 \pm 0.022	0.3659 \pm 0.0115 (+)	0.0827 \pm 0.0021 (+)
MMF15 (5)	0.4959 \pm 0.0076	0.5600 \pm 0.0155 (+)	0.5172 \pm 0.0014 (+)	0.1559 \pm 0.0014	0.4118 \pm 0.0152 (+)	0.1602 \pm 0.0005 (~)	0.0000 \pm 0.0000	43.6883 \pm 3.9734 (+)	0.0000 \pm 0.0000 (~)	0.0654 \pm 0.0017	0.4610 \pm 0.0152 (+)	0.0625 \pm 0.0025 (~)
MMF15_a (5)	0.4969 \pm 0.0086	0.5660 \pm 0.0155 (+)	0.5232 \pm 0.0071 (+)	0.1783 \pm 0.0062	0.3672 \pm 0.0128 (+)	0.1938 \pm 0.0078 (+)	0.0000 \pm 0.0000	45.3237 \pm 3.4695 (+)	0.9428 \pm 0.8165 (+)	0.0954 \pm 0.0045	0.4339 \pm 0.0162 (+)	0.0961 \pm 0.0053 (~)
MMF14 (8)	0.2772 \pm 0.0012	0.5663 \pm 0.0129 (+)	0.3088 \pm 0.0018 (+)	0.4025 \pm 0.0011	0.4386 \pm 0.0070 (+)	0.4178 \pm 0.0011 (+)	0.0000 \pm 0.0000	101.1673 \pm 4.3256 (+)	5.3833 \pm 0.0000 (+)	0.1332 \pm 0.0002	0.6277 \pm 0.0154 (+)	0.1456 \pm 0.0016 (+)
MMF14_a (8)	0.2796 \pm 0.0008	0.5588 \pm 0.0114 (+)	0.2900 \pm 0.0062 (+)	0.4222 \pm 0.0004	0.4480 \pm 0.0045 (+)	0.4335 \pm 0.0021 (+)	0.0000 \pm 0.0000	106.8644 \pm 3.5223 (+)	5.3833 \pm 0.0000 (+)	0.1742 \pm 0.0044	0.5917 \pm 0.0149 (+)	0.1817 \pm 0.0044 (+)
MMF15 (8)	0.2524 \pm 0.0002	0.6438 \pm 0.0175 (+)	0.2713 \pm 0.0018 (+)	0.3537 \pm 0.0052	0.5312 \pm 0.0059 (+)	0.3815 \pm 0.0015 (+)	0.0000 \pm 0.0000	99.5550 \pm 3.0343 (+)	5.4810 \pm 0.1382 (+)	0.1288 \pm 0.0038	0.6767 \pm 0.0128 (+)	0.1508 \pm 0.0008 (+)
MMF15_a (8)	0.2430 \pm 0.0137	0.6113 \pm 0.0093 (+)	0.2688 \pm 0.0027 (+)	0.3797 \pm 0.0115	0.4885 \pm 0.0078 (+)	0.3886 \pm 0.0068 (~)	0.0000 \pm 0.0000	103.5948 \pm 3.5180 (+)	5.5787 \pm 0.0000 (+)	0.2014 \pm 0.0025	0.6488 \pm 0.0151 (+)	0.2122 \pm 0.0284 (+)
MMF14 (10)	0.2595 \pm 0.0005	0.5880 \pm 0.0101 (+)	0.2620 \pm 0.0038 (+)	0.5088 \pm 0.0087	0.5584 \pm 0.0046 (+)	0.5356 \pm 0.0085 (+)	0.141331 \pm 2.5516	141.331 \pm 4.6720 (+)	38.9838 \pm 0.7255 (+)	0.2200 \pm 0.0037	0.6575 \pm 0.0129 (+)	0.2504 \pm 0.0002 (+)
MMF14_a (10)	0.2717 \pm 0.0106	0.5930 \pm 0.0134 (+)	0.2718 \pm 0.0083 (~)	0.5165 \pm 0.0008	0.5699 \pm 0.0036 (+)	0.5393 \pm 0.0063 (+)	21.9299 \pm 0.4837	137.8081 \pm 3.8224 (+)	41.7357 \pm 0.5083 (+)	0.2554 \pm 0.0065	0.6311 \pm 0.0128 (+)	0.2966 \pm 0.0041 (+)
MMF15 (10)	0.2557 \pm 0.0023	0.6590 \pm 0.0123 (+)	0.2481 \pm 0.0030 (~)	0.4516 \pm 0.0096	0.6180 \pm 0.0071 (+)	0.4850 \pm 0.0005 (~)	17.6340 \pm 1.4436	131.8568 \pm 4.0914 (+)	36.4571 \pm 9.3681 (+)	0.2219 \pm 0.0118	0.7072 \pm 0.0109 (+)	0.2535 \pm 0.0072 (+)
MMF15_a (10)	0.2664 \pm 0.0143	0.6350 \pm 0.0119 (+)	0.2652 \pm 0.0098 (~)	0.4731 \pm 0.0061	0.5780 \pm 0.0048 (+)	0.4903 \pm 0.0006 (+)	23.2171 \pm 2.4365	133.7104 \pm 2.8705 (+)	39.7423 \pm 1.7614 (+)	0.2672 \pm 0.0037	0.6812 \pm 0.0092 (+)	0.3193 \pm 0.0007 (+)
Sum-up	+/-/~	15/0/1	13/1/2	+/-/~	16/0/0	13/0/3	+/-/~	16/0/0	10/0/6	+/-/~	16/0/0	9/1/6

As a result, for some MMMOPs, such as MMF11 and MMF12, it has very poor performance. Since, by using cluster-wise SCD, LORD addresses the crowding illusion problem (Section 2, Fig. 2), it has superior performance in most cases in both decision as well as in objective space.

- Even with the increase in the number of subsets in the global PS (#Sets in Table 1), the performance of LORD remains steady (Tables 3 and 4).
- It is important for MMOEAs to converge to global optima of MMMOPs, overcoming the local optima. As LORD gives satisfactory performance for MMF10 to MMF13, which are problems with one global PS, LORD can also be considered to serve as an excellent MOEA.
- rPSP is the ratio of IGDX to cover rate (cov_rate) where cover rate indicates the proportion of overlapping region between the obtained and true bounds of the decision variables [23]. As cov_rate is nearly equal to one (ideal value) for the test results, Table 3 reflect similar values of rPSP and IGDX.

Due to space constraint, the plots of PS and PF (for the median run) obtained by LORD are presented in Section V of the supplementary material and compared with

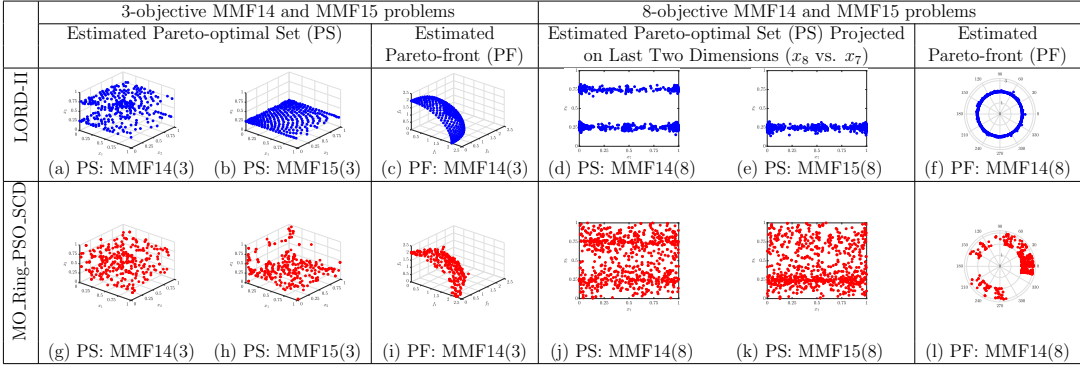


Figure 5: Visualizations of Pareto-optimal Set (PS) and Pareto-Front (PF) of 3- and 8-objective MMF14 and MMF15 problems for median runs by LORD-II (top row) and MO_Ring_PSO_SCD (bottom row). As both MMF14 and MMF15 problems have similar PF, only the obtained PF of MMF14 are shown here.

those obtained by MO_Ring_PSO_SCD and the ground truth.

The following insights can be obtained for LORD-II from the results presented in Table 5:

- For 3-objective problems, LORD-II and MOEA/DD has similar performance in the objective space. However, both the EAs outperform MO_Ring_PSO_SCD by a large margin in convergence (CM) and diversity (D_metric). In the decision space, LORD-II maintains superiority.
- For 5-objective problems, LORD-II outperforms both the EAs in the decision space. However, LORD-II and MOEA/DD have similar performance in two cases, LORD-II is superior in one case and marginally outperformed in another case by MOEA/DD.
- For 8- and 10-objective problems, LORD-II exhibits superior performance in both decision and objective space.
- As seen from Fig. 5, PS and PF estimated by LORD-II have not only converged to global optimal surfaces but also the solutions are uniformly spread. The performance by MO_Ring_PSO_SCD (Fig. 5) is not as good as LORD-II and deteriorates severely with increase in dimension. The radial plot visualization of the estimated PF [38, 46] shows that for LORD-II (Fig. 5f), all solutions have approximately converged to the global PF and form a uniformly distributed circle. This is not the case for MO_Ring_PSO_SCD (Fig. 5l) and hence, it yields poor values in the objective space.

The scalability of the proposed approach for exploration of solution distribution in the decision space is established in Section VI of the supplementary material where the performance of LORD-II is analyzed by varying the dimension of the decision space i.e., with $N = \{3, 10, 30, 50, 100\}$ for the 3-objective MMF14 problem. Another experiment demonstrates the superior diversity attainment behavior (in both decision and objective spaces) of LORD in Section VII of the supplementary material.

5 Conclusion and Future Research Directions

In this work, a novel EA is presented which deals with the challenges of MMMOPs. It is a first of its kind algorithm to attempt decomposition of decision space using graph Laplacian based clustering for maintaining the diversity of solutions in that space. It uses reference vectors to partition the objective space for maintaining diversity in the objective space. The proposed algorithm has two different versions to entail the convergence attribute. The first version (LORD) is for MMMOPs with small number of objectives, which eliminates the maximally crowded solution from the last non-dominated rank. The second version (LORD-II) is for problems with higher number of objectives which eliminates the candidate with maximal PBI, from the maximally large cluster. During elimination of candidate, LORD and LORD-II try to ensure that the removal does not occur from the sub-spaces (defined by reference vectors) with only one associated candidate. The proposed frameworks have been tested over 34 test instances from the CEC 2019 test suite for MMMOPs [4] and their performance have been compared with recent state-of-the-art algorithms to establish their efficacy.

Inspite of their superior performance, LORD and LORD-II have the following disadvantages; reducing the effects of which could be considered for future extensions of this work:

1. Spectral clustering solves the preliminary purpose of decomposing the decision space and is effective for problems like MMF2, MMF3, SYM-PART, etc. However, for problems like MMF1, MMF6, MMF7, etc., where overlap exists along certain dimensions within each subset of PS [4], spectral clustering does not completely eliminate the crowding illusion problem (Fig. 2). Hence, the search for better decomposition methods in the decision space forms a potential future work.
2. As done in the proposed work as well as in most of the previous works such as [8,25], the mating pool selection is performed from neighboring candidates in the objective space. Nonetheless, if an approximate partitioning of the decision space could be done to yield the bounding box of each subset of PS, intra- and inter-subset mating could further be studied for enhanced diversity of solutions

in the decision space. Moreover, different subsets of the PS of an MMMOP have correlated structures. Such information on correlation could be incorporated to design new perturbation operators for guiding the search in MMMOPs.

3. It should be noted that the research on MMMOPs has just started developing. Hence, besides designing more algorithms to deal with MMMOPs, other challenges in this new direction involve developing novel decision-making strategies (selecting one out of multiple equivalent solutions from the PS mapping to a certain solution in the PF), analyzing more practical problems, designing benchmark problems replicating real-world challenges as well as designing new performance measures (independent of the true PS) to study the convergence and diversity in the decision space for practical problems.

References

- [1] C. A. C. Coello. Recent results and open problems in evolutionary multiobjective optimization. In C. Martín-Vide, R. Neruda, and M. A. Vega-Rodríguez, editors, *Theory and Practice of Natural Computing*, pages 3–21, Cham, 2017. Springer International Publishing.
- [2] Anirban Mukhopadhyay, Ujjwal Maulik, Sanghamitra Bandyopadhyay, and Carlos Artemio Coello Coello. A survey of multiobjective evolutionary algorithms for data mining: Part I. *IEEE Transactions on Evolutionary Computation*, 18(1):4–19, Feb 2014.
- [3] Ryoji Tanabe and Hisao Ishibuchi. A review of evolutionary multi-modal multi-objective optimization. *IEEE Transactions on Evolutionary Computation*, pages 1–9, 2019.
- [4] J. J. Liang, B. Y. Qu, D. W. Gong, and C. T. Yue. Problem definitions and evaluation criteria for the CEC special session on multimodal multiobjective optimization. *Technical Report, Computational Intelligence Laboratory, Zhengzhou University*, 2019.
- [5] Fumiya Kudo, Tomohiro Yoshikawa, and Takeshi Furuhashi. A study on analysis of design variables in pareto solutions for conceptual design optimization problem of hybrid rocket engine. In *2011 IEEE Congress of Evolutionary Computation (CEC)*, pages 2558–2562, June 2011.
- [6] C. T. Yue, J. J. Liang, B. Y. Qu, K. J. Yu, and H. Song. Multimodal multiobjective optimization in feature selection. In *2019 IEEE Congress on Evolutionary Computation (CEC)*, pages 302–309, June 2019.

- [7] Jafar Jamal, Roberto Montemanni, David Huber, Marco Derboni, and Andrea E Rizzoli. A multi-modal and multi-objective journey planner for integrating car-pooling and public transport. *Journal of Traffic and Logistics Engineering*, 5(2):68–72, December 2017.
- [8] Monalisa Pal and Sanghamitra Bandyopadhyay. Differential evolution for multi-modal multi-objective problems. In *Proceedings of the Genetic and Evolutionary Computation Conference Companion*, GECCO ’19, pages 1399–1406, New York, NY, USA, 2019. ACM.
- [9] K. Deb, A. Pratap, S. Agarwal, and T. Meyarivan. A fast and elitist multiobjective genetic algorithm: NSGA-II. *IEEE Transactions on Evolutionary Computation*, 6(2):182–197, 2002.
- [10] Y. Yuan, X. Hua, W. Bo, and Y. Xin. A new dominance relation-based evolutionary algorithm for many-objective optimization. *IEEE Transactions on Evolutionary Computation*, 20(1):16–37, 2016.
- [11] J. Bader and E. Zitzler. HypE: An algorithm for fast hypervolume-based many-objective optimization. *Evolutionary computation*, 19(1):45–76, 2011.
- [12] Adriana Menchaca-Mendez and Carlos A Coello Coello. GDE-MOEA: a new moea based on the generational distance indicator and ε -dominance. In *2015 IEEE Congress on Evolutionary Computation (CEC)*, pages 947–955. IEEE, 2015.
- [13] Z. Qingfu and L. Hui. MOEA/D: A multiobjective evolutionary algorithm based on decomposition. *IEEE Transactions on Evolutionary Computation*, 11(6):712–731, 2007.
- [14] Kalyanmoy Deb and Himanshu Jain. An evolutionary many-objective optimization algorithm using reference-point-based nondominated sorting approach, part I: Solving problems with box constraints. *IEEE Transactions on Evolutionary Computation*, 18(4):577–601, 2014.
- [15] Ke Li, Kalyanmoy Deb, Qingfu Zhang, and Sam Kwong. An evolutionary many-objective optimization algorithm based on dominance and decomposition. *IEEE Transactions on Evolutionary Computation*, 19(5):694–716, 2015.
- [16] I. Das and J. E. Dennis. Normal-boundary intersection: A new method for generating the pareto surface in nonlinear multicriteria optimization problems. *SIAM Journal on Optimization*, 8(3):631–657, 1998.

- [17] Qi Kang, Xinyao Song, MengChu Zhou, and Li Li. A collaborative resource allocation strategy for decomposition-based multiobjective evolutionary algorithms. *IEEE Transactions on Systems, Man, and Cybernetics: Systems*, 49(12):2416–2423, Dec 2019.
- [18] Kalyanmoy Deb and Santosh Tiwari. Omni-optimizer: A procedure for single and multi-objective optimization. In Carlos A. Coello Coello, Arturo Hernández Aguirre, and Eckart Zitzler, editors, *Evolutionary Multi-Criterion Optimization*, pages 47–61, Berlin, Heidelberg, 2005. Springer Berlin Heidelberg.
- [19] K. P. Chan and T. Ray. An evolutionary algorithm to maintain diversity in the parametric and the objective space. In *International Conference on Computational Robotics and Autonomous Systems (CIRAS)*, Centre for Intelligent Control, National University of Singapore, 2005.
- [20] Aimin Zhou, Qingfu Zhang, and Yaochu Jin. Approximating the set of pareto-optimal solutions in both the decision and objective spaces by an estimation of distribution algorithm. *IEEE Transactions on Evolutionary Computation*, 13(5):1167–1189, 2009.
- [21] J. J. Liang, C. T. Yue, and B. Y. Qu. Multimodal multi-objective optimization: A preliminary study. In *2016 IEEE Congress on Evolutionary Computation (CEC)*, pages 2454–2461. IEEE, 2016.
- [22] Mahrokh Javadi, Heiner Zille, and Sanaz Mostaghim. Modified crowding distance and mutation for multimodal multi-objective optimization. In *Proceedings of the Genetic and Evolutionary Computation Conference Companion*, GECCO ’19, pages 211–212, New York, NY, USA, 2019. ACM.
- [23] Caitong Yue, Boyang Qu, and Jing Liang. A multiobjective particle swarm optimizer using ring topology for solving multimodal multiobjective problems. *IEEE Transactions on Evolutionary Computation*, 22(5):805–817, Oct 2018.
- [24] Qinjin Fan and Xuefeng Yan. Solving multimodal multiobjective problems through zoning search. *IEEE Transactions on Systems, Man, and Cybernetics: Systems*, pages 1–12, 2019.
- [25] Ryoji Tanabe and Hisao Ishibuchi. A decomposition-based evolutionary algorithm for multi-modal multi-objective optimization. In Anne Auger, Carlos M. Fonseca, Nuno Lourenço, Penousal Machado, Luís Paquete, and Darrell Whitley, editors, *Parallel Problem Solving from Nature – PPSN XV*, pages 249–261, Cham, 2018. Springer International Publishing.

- [26] Yiping Liu, Gary G. Yen, and Dunwei Gong. A multi-modal multi-objective evolutionary algorithm using two-archive and recombination strategies. *IEEE Transactions on Evolutionary Computation*, 23(4):660–674, Aug 2019.
- [27] K. Maity, R. Sengupta, and S. Saha. MM-NAEMO : Multimodal neighborhood-sensitive archived evolutionary many-objective optimization algorithm. In *2019 IEEE Congress on Evolutionary Computation (CEC)*, pages 286–294, June 2019.
- [28] Ryoji Tanabe and Hisao Ishibuchi. A niching indicator-based multi-modal many-objective optimizer. *Swarm and Evolutionary Computation*, 49:134 – 146, 2019.
- [29] Raunak Sengupta, Monalisa Pal, Sriparna Saha, and Sanghamitra Bandyopadhyay. NAEMO: Neighborhood-sensitive archived evolutionary many-objective optimization algorithm. *Swarm and Evolutionary Computation*, 46:201 – 218, 2019.
- [30] Li-Min Li, Kang-Di Lu, Guo-Qiang Zeng, Lie Wu, and Min-Rong Chen. A novel real-coded population-based extremal optimization algorithm with polynomial mutation: A non-parametric statistical study on continuous optimization problems. *Neurocomputing*, 174:577 – 587, 2016.
- [31] Xianpeng Wang, Zhiming Dong, and Lixin Tang. Multiobjective differential evolution with personal archive and biased self-adaptive mutation selection. *IEEE Transactions on Systems, Man, and Cybernetics: Systems*, pages 1–13, 2018.
- [32] T. Robič and B. Filipič. DEMO: Differential evolution for multiobjective optimization. In C. A. C. Coello, A. H. Aguirre, and E. Zitzler, editors, *Evolutionary Multi-Criterion Optimization*, pages 520–533, Berlin, Heidelberg, 2005. Springer Berlin Heidelberg.
- [33] Ulrike von Luxburg. A tutorial on spectral clustering. *Statistics and Computing*, 17(4):395–416, Dec 2007.
- [34] Jeff Cheeger. A lower bound for the smallest eigenvalue of the Laplacian. In Robert C. Gunning, editor, *Problems in analysis (Papers dedicated to Salomon Bochner, 1969)*, pages 195–199. Princeton Univ. Press, Princeton, NJ, 1970.
- [35] Peter Buser. Über eine ungleichung von Cheeger (On an inequality of Cheeger). *Mathematische Zeitschrift (in German)*, 158(3):245–252, Oct 1978.
- [36] Michael B. Cohen, Sam Elder, Cameron Musco, Christopher Musco, and Madalina Persu. Dimensionality reduction for k-means clustering and low rank approximation. In *Proceedings of the Forty-seventh Annual ACM Symposium on*

Theory of Computing, STOC '15, pages 163–172, New York, NY, USA, 2015. ACM.

- [37] Sumit Mishra, Mondal. Samrat, and Sriparna Saha. Fast implementation of steady-state NSGA-II. In *2016 IEEE Congress on Evolutionary Computation (CEC)*, pages 3777–3784, July 2016.
- [38] Monalisa Pal and Sanghamitra Bandyopadhyay. ESOEA: Ensemble of single objective evolutionary algorithms for many-objective optimization. *Swarm and Evolutionary Computation*, 2019.
- [39] S. Bandyopadhyay and A. Mukherjee. An algorithm for many-objective optimization with reduced objective computations: A study in differential evolution. *IEEE Transactions on Evolutionary Computation*, 19(3):400–413, 2015.
- [40] M. Pal and S. Bandyopadhyay. Reliability of convergence metric and hyper-volume indicator for many-objective optimization. In *Control, Instrumentation, Energy & Communication (CIEC), 2016 2nd International Conference on*, pages 511–515. IEEE, Jan 2016.
- [41] Raunak Sengupta, Monalisa Pal, Sriparna Saha, and Sanghamitra Bandyopadhyay. Population dynamics indicators for evolutionary many-objective optimization. In Chhabi Rani Panigrahi, Arun K. Pujari, Sudip Misra, Bibudhendu Pati, and Kuan-Ching Li, editors, *Progress in Advanced Computing and Intelligent Engineering*, pages 261–271 (in Press), Singapore, 2019. Springer Singapore.
- [42] Ye Tian, Ran Cheng, Xingyi Zhang, Fan Cheng, and Yaochu Jin. An indicator based multi-objective evolutionary algorithm with reference point adaptation for better versatility. *IEEE Transactions on Evolutionary Computation*, 2017.
- [43] Ye Tian, Xingyi Zhang, Ran Cheng, and Yaochu Jin. A multi-objective evolutionary algorithm based on an enhanced inverted generational distance metric. In *2016 IEEE Congress on Evolutionary Computation (CEC)*, pages 5222–5229, July 2016.
- [44] Anirban Mukhopadhyay, Ujjwal Maulik, Sanghamitra Bandyopadhyay, and Carlos Artemio Coello Coello. Survey of multiobjective evolutionary algorithms for data mining: Part II. *IEEE Transactions on Evolutionary Computation*, 18(1):20–35, Feb 2014.
- [45] Hisao Ishibuchi, Naoya Akedo, and Yusuke Nojima. A many-objective test problem for visually examining diversity maintenance behavior in a decision space. In

- Proceedings of the 13th Annual Conference on Genetic and Evolutionary Computation*, GECCO '11, pages 649–656, New York, NY, USA, 2011. ACM.
- [46] Z. He and G. G. Yen. An improved visualization approach in many-objective optimization. In *2016 IEEE Congress on Evolutionary Computation (CEC)*, pages 1618–1625. IEEE, 2016.

Supplementary Material for Decomposition in Decision and Objective Space for Multi-Modal Multi-Objective Optimization

Monalisa Pal and Sanghamitra Bandyopadhyay*

1 Introduction

This is a supplementary document for the article proposing graph Laplacian based Optimization using Reference vector assisted Decomposition (LORD) for Multi-Modal Multi-objective Optimization Problems (MMMOPs) [1] and its extension (LORD-II) for multi-modal many-objective optimization problems. This material is to assist the readers to obtain a deeper insight on various topics associated with the proposed approach. Kindly note that this is not a stand-alone document and bears reference to the main article proposing LORD and LORD-II.

This material consists of the following topics in its different sections:

1. Section 2 of this material describes the various performance indicators used to analyze the performance of LORD and LORD-II in the proposed work.
2. Section 3 of this material presents an experiment to study the sensitivity of thresholding for nearest neighbor graph formation which assists in spectral clustering (decomposition) of the decision space for LORD and LORD-II. It also presents an experiment to study the sensitivity of the probability (threshold) for switching between different reproduction strategies (DE/rand/1/bin and SBX crossover).

*M. Pal and S. Bandyopadhyay are with Machine Intelligence Unit, Indian Statistical Institute, 203 Barrackpore Trunk Road, Kolkata - 700108, West Bengal, India. E-mail: M. Pal (monalisa.pal.r@isical.ac.in) and S. Bandyopadhyay (sanghami@isical.ac.in). This work is partially supported by Indian Statistical Institute, Kolkata and by J. C. Bose Fellowship (SB/SJ/JCB-033/2016) of Department of Science and Technology, Government of India.

3. Section 4 compares the performance of LORD and LORD-II with six other multi-modal multi-objective evolutionary algorithms (MMMOEAs) which were designed for specific types of multi-modal multi-objective problems (MMMOPs).
4. Section 5 provides the Cartesian coordinate plots of the Pareto-optimal sets (PSs) and the Pareto-fronts (PFs) of the 22 test instances of CEC 2019 test suite [2] and compares them with those obtained by MO_Ring_PSO_SCD (a state-of-the-art algorithm for MMMOPs) [3] and LORD (or LORD-II).
5. Section 6 of this material presents a scalability study on the performance of LORD-II for addressing 3-objective MMF14 problem up to 100 candidate dimensions.
6. Section 7 of this material analyzes the diversity attainment behavior of LORD in both objective space and decision space.
7. Finally, the material is concluded in Section 8.

2 Brief Description of Performance Indicators

This section briefly describes the various performance indicators used to analyze the performance of LORD and LORD-II in the proposed work.

2.1 Convergence Metric

Convergence Metric [4, 5] (also known as generational distance [6]) indicates the convergence of the solutions in the estimated Pareto-optimal surface to the true Pareto-optimal surface. Let \mathcal{A} be a non-dominated set of solutions and \mathcal{H}_{CM} be a set of several points sampled uniformly across the Pareto-optimal surface. Convergence metric (CM) is estimated by (1) as the sample mean of the minimum Euclidean distance $D_E(\cdot)$ of the objective vectors estimating the Pareto-Front ($\mathcal{A}_F = \{\mathbf{F}(\mathbf{X}_i) | \mathbf{X}_i \in \mathcal{A}\}$) from the points in the reference set ($\mathbf{H}_j \in \mathcal{H}_{CM}$), over the number of solutions in the approximated Pareto-Front. If CM is evaluated in the decision space \mathcal{H}_{CM} is a representation of the true Pareto-optimal Set and instead of $\mathbf{F}(\mathbf{X}_i) \in \mathcal{A}_F$, $\mathbf{X}_i \in \mathcal{A}$ is considered in (1).

$$CM(\mathcal{A}_F, \mathcal{H}_{CM}) = \frac{1}{|\mathcal{A}_F|} \sum_{i=1}^{|\mathcal{A}_F|} \left(\min_{j=1}^{|\mathcal{H}_{CM}|} (D_E(\mathbf{F}(\mathbf{X}_i), \mathbf{H}_j)) \right), \quad (1)$$

where $\mathbf{F}(\mathbf{X}_i) \in \mathcal{A}_F$ and $\mathbf{H}_j \in \mathcal{H}_{CM}$

2.2 Inverted Generational Distance

Inverted Generational Distance (IGD) [7,8] gives an indication of the convergence as well as the diversity of the approximated Pareto-Front. Let \mathcal{A} be a non-dominated set of solutions and $\mathcal{A}_F = \{\mathbf{F}(\mathbf{X}_i) | \mathbf{X}_i \in \mathcal{A}\}$ be the estimated Pareto-Front. Similar to the evaluation of CM , IGD also requires a set \mathcal{H}_{IGD} of N_{IGD} points sampled uniformly over the true Pareto-Front (if evaluated in the objective space). IGD is estimated by (2) as the sample mean of the minimum Euclidean distance $D_E(\cdot)$ of the points in the reference set ($\mathbf{H}_j \in \mathcal{H}_{IGD}$) from the objective vectors constituting the approximated Pareto-Front ($\mathbf{F}(\mathbf{X}_i) \in \mathcal{A}_F$), over the number of solutions in \mathcal{H}_{IGD} . If IGD is evaluated in the decision space \mathcal{H}_{IGD} is a representation of the true Pareto-optimal Set and instead of $\mathbf{F}(\mathbf{X}_i) \in \mathcal{A}_F$, $\mathbf{X}_i \in \mathcal{A}$ is considered in (2). In this work, IGDF is used to represent IGD in objective space and IGDX is used to represent IGD in decision space.

$$IGD(\mathcal{A}_F, \mathcal{H}_{IGD}) = \frac{1}{|\mathcal{H}_{IGD}|} \sum_{j=1}^{|\mathcal{H}_{IGD}|} \left(\min_{i=1}^{|\mathcal{A}_F|} (D_E(\mathbf{F}(\mathbf{X}_i), \mathbf{H}_j)) \right), \quad (2)$$

where $\mathbf{F}(\mathbf{X}_i) \in \mathcal{A}_F$ and $\mathbf{H}_j \in \mathcal{H}_{IGD}$

2.3 Hypervolume Indicator

Hypervolume Indicator [4,9] can also represent both convergence and diversity information using a single value and also its evaluation is independent of the knowledge of the true Pareto-Front. For its evaluation, a hyper-rectangle is considered between a reference point (\mathbf{R}_{HV}) and the origin of the objective space. A set of points (say \mathcal{H}_{HV}) is randomly sampled in this hyper-rectangle using Monte-Carlo simulation. Hypervolume Indicator (HV) is given by (3) which yields the fraction of the points in \mathcal{H}_{HV} which are Pareto-dominated by the non-dominated set of solutions, approximating the Pareto-Front (denoted by \mathcal{A}_F). For its evaluation, an attainment function ($\alpha_{HV}(\cdot)$) is defined which returns 1 when a point $\mathbf{H}_j \in \mathcal{H}_{HV}$ is dominated by any solution ($\mathbf{F}(\mathbf{X}_i) \in \mathcal{A}_F$). Hypervolume Indicator is given by the average of the values returned by the attainment function over the set of points belonging to \mathcal{H}_{HV} .

$$HV(\mathcal{A}_F, \mathcal{H}_{HV}) = \frac{1}{|\mathcal{H}_{HV}|} \sum_{j=1}^{|\mathcal{H}_{HV}|} \alpha_{HV}(\mathbf{H}_j, \mathcal{A}_F), \quad (3)$$

where $\mathbf{H}_j \in \mathcal{H}_{HV}$ and $\alpha_{HV}(\mathbf{H}_j, \mathcal{A}_F) =$

$$\begin{cases} 1, & \text{if } \exists \mathbf{F}(\mathbf{X}_i) \in \mathcal{A}_F \text{ with } \mathbf{F}(\mathbf{X}_i) \prec \mathbf{H}_j \\ 0, & \text{otherwise} \end{cases}$$

2.4 Pareto-Set Proximity

Pareto-Set Proximity (PSP) [3] is used to evaluate the similarity between the approximated Pareto-optimal Set (\mathcal{A}) and the true Pareto-optimal Set (represented by a set \mathcal{H}_{IGD} of N_{IGD} points sampled uniformly on the true Pareto-optimal Set). PSP is given by (4) where *cov_rate* represents the cover rate (overlap ratio of the approximated Pareto-optimal Set to the true Pareto-optimal Set) and $IGD(\mathcal{A}, \mathcal{H}_{IGD})$ represents IGD_X. In (4), x_i^{min} and x_i^{max} represent the minimum and maximum along the i^{th} decision variable over the approximated Pareto-optimal Set, respectively. Similarly, x_i^{MIN} and x_i^{MAX} represent the minimum and maximum along the i^{th} decision variable over the true Pareto-optimal Set¹, respectively. While *cov_rate* indicates overlap, $IGD(\mathcal{A}, \mathcal{H}_{IGD})$ represents convergence and diversity of the approximated Pareto-optimal Set with respect to true Pareto-optimal Set. Thus, PSP quantifies an overall quality of the approximated Pareto-optimal Set.

$$\begin{aligned}
PSP(\mathcal{A}, \mathcal{H}_{IGD}) &= \frac{\text{cov_rate}}{IGD(\mathcal{A}, \mathcal{H}_{IGD})} \\
\text{where cov_rate} &= \left(\prod_{i=1}^N \gamma_i \right)^{\frac{1}{2N}}, \\
\gamma_i &= \begin{cases} 1, & \text{if } x_i^{MAX} = x_i^{MIN} \\ 0, & \text{if } x_i^{min} \geq x_i^{MAX} \vee x_i^{max} \leq x_i^{MIN} \\ z_i, & \text{otherwise} \end{cases} \\
\text{and } z_i &= \left(\frac{\min(x_i^{max}, x_i^{MAX}) - \max(x_i^{min}, x_i^{MIN})}{x_i^{MAX} - x_i^{MIN}} \right)^2
\end{aligned} \tag{4}$$

2.5 Diversity indicator: D-metric

This indicator is a measure of the diversity of the population in the objective space [10]. Let S_k^G represent the number of objective vectors associated with the k^{th} reference vector at generation G . Ideal value of $S_k^G = S_{ideal}^G = n_{pop}/n_{dir}$ where n_{pop} is the size of the population and n_{dir} is the number of reference vectors. At generation G , D_metric^G is defined by (5) which has an ideal value of zero implying best diversity. A higher value of D_metric implies poor diversity. Thus, D_metric of the population at termination of an EA is gives the diversity attained by the estimated

¹It should be noted x_i^{MIN} and x_i^{MAX} are the bounds of the i^{th} variable over true Pareto-optimal Set, not over the decision space \mathcal{D} .

Pareto-Front [10].

$$D_metric^G = \frac{n_{dir}}{n_{pop}} \sqrt{\sum_{k=1}^{n_{dir}} (S_k^G - S_{ideal}^G)^2} \quad (5)$$

2.6 Non-Contributing Solutions and Associated Indicators

As seen from (2), IGDX evaluation involves the term $\min_{\mathbf{X}_i \in \mathcal{A}} (D_E(\mathbf{X}_i, \mathbf{H}_j))$ where $\mathbf{H}_j \in \mathcal{H}_{IGD}$. A solution $\mathbf{X}_i^{NS} \in \mathcal{A}$ is called a non-contributing solution, if for a given representation of the true Pareto-optimal Set (\mathcal{H}_{IGD}) and a given set of non-dominated solutions (\mathcal{A}) the condition in (6) is satisfied [6, 11].

$$\#\mathbf{H}_j \in \mathcal{H}_{IGD} : D_E(\mathbf{X}_i^{NS}, \mathbf{H}_j) = \min_{\mathbf{X}_i \in \mathcal{A}} (D_E(\mathbf{X}_i, \mathbf{H}_j)) \quad (6)$$

Let the subset of the non-dominated solution set consisting of all such non-contributing solutions be \mathcal{A}^{NS} . The proportion of non-contributing solutions in the non-dominated solution set is given by $NSX = |\mathcal{A}^{NS}| / |\mathcal{A}|$. In this work, this proportion NSX is reported as an indicator to reflect the amount of outliers i.e., how many non-dominated solutions of the final population are not the nearest neighbors of any point in \mathcal{H}_{IGD} (the set representing the true Pareto-optimal Set).

Removing \mathcal{A}^{NS} from \mathcal{A} does not change IGDX i.e., $IGD(\mathcal{A}, \mathcal{H}_{IGD}) = IGD(\mathcal{A} - \mathcal{A}^{NS}, \mathcal{H}_{IGD})$. However, to note how far the outliers are from the surface of true Pareto-optimal Set, in this work, the convergence metric of \mathcal{A}^{NS} is evaluated in the decision space with respect to \mathcal{H}_{CM} i.e., $CM_NSX = CM(\mathcal{A}^{NS}, \mathcal{H}_{CM})$. If both NSX and CM_NSX are large, it implies that a large number of solutions are far away from the true Pareto-optimal Set.

3 Parameter Sensitivity Studies

3.1 Parameter: Threshold for Nearest Neighbor Graph

One of the major strategies of the proposed evolutionary frameworks is the spectral clustering of the decision space (Section III-B of the main manuscript). The first step of spectral clustering involves formation of the nearest neighbor graph. For constructing this graph, distances between every pair of candidates (nodes) are obtained and edges are placed between nodes whose distance is less than a threshold of ε_L . In Section IV-C of the main manuscript, it is stated that ε_L is considered as α_L ($= 0.2$) times the longest possible distance in the decision space i.e., diagonal of the box-constrained decision space, \mathcal{D} .

Table 1: Mean of IGDX and IGDF for some MMMOPs over 51 Independent Runs of LORD and LORD-II for Sensitivity Study of α_L .

	$\alpha_L \rightarrow$	IGDX				IGDF			
		0.1	0.2	0.5	0.8	0.1	0.2	0.5	0.8
LORD	MMF1	0.0504	0.0431	0.0479	0.0492	0.0028	0.0025	0.0025	0.0028
	MMF2	0.1431	0.0180	0.0304	0.0366	0.0092	0.0070	0.0109	0.0173
	MMF3	0.0459	0.0176	0.0419	0.0458	0.0084	0.0069	0.0103	0.0117
	MMF4	0.0298	0.0251	0.0303	0.0352	0.0021	0.0018	0.0023	0.0024
	MMF5	0.0976	0.0814	0.0943	0.1165	0.0025	0.0024	0.0025	0.0027
	MMF6	0.0812	0.0692	0.0720	0.0890	0.0025	0.0023	0.0024	0.0024
	MMF7	0.0277	0.0218	0.0299	0.0339	0.0024	0.0022	0.0026	0.0028
	MMF8	0.1631	0.0762	0.1299	0.1577	0.0025	0.0025	0.0025	0.0025
LORD-II	MMF14	0.0495	0.0443	0.0522	0.0580	0.0550	0.0540	0.0545	0.0546
	MMF14_a	0.0657	0.0576	0.0665	0.0674	0.0574	0.0561	0.0582	0.0583
	MMF15	0.0295	0.0287	0.0292	0.0293	0.0552	0.0548	0.0552	0.0558
	MMF15_a	0.0369	0.0355	0.0373	0.0379	0.0584	0.0571	0.0589	0.0593

In this section of the supplementary material, α_L is varied between 0.1 to 0.8 such that ε_L is varied between 10% to 80% of the length diagonal of \mathcal{D} . The performance of LORD with different thresholds for nearest neighbor graph is studied in terms of IGDX and IGDF for MMF1 to MMF8 problems. Similarly, the performance of LORD-II is studied for 3-objective MMF14, MMF14_a, MMF15 and MMF15_a problems.

It can be seen from Table 1 that the best performance is obtained at $\alpha_L = 0.2$. With increasing threshold, all the points in the decision space form a single component and distinguishability of multiple PSs is lost which deteriorates the performance. On the other hand, when the threshold is very small, the number of clusters becomes approximately equal to the population size and every candidate is treated independently. This leads to higher randomness and thus, degrades the performance of the proposed evolutionary frameworks.

3.2 Parameter: Threshold for Reproduction Switching

Another characteristic feature of the proposed evolutionary frameworks is the probabilistic switching between two reproduction strategies for perturbation of candidates (Algorithm 3 of the main manuscript). This switching is dictated by a threshold (P_{mut}) which decides whether DE/rand/1/bin [12] or SBX-crossover [13] is followed. A lower value of P_{mut} implies DE/rand/1/bin is favoured over SBX-crossover. In Section IV-C of the main manuscript, it is stated that $P_{mut} = 0.25$ is considered.

In this section of the supplementary material, P_{mut} is tested for the following

Table 2: Mean of IGDX and IGDF for some MMMOPs over 51 Independent Runs of LORD and LORD-II for Sensitivity Study of P_{mut} .

	$P_{mut} \rightarrow$	IGDX					IGDF				
		0.00	0.25	0.50	0.75	1.00	0.00	0.25	0.50	0.75	1.00
LORD	MMF1	0.0529	0.0431	0.0470	0.0472	0.0506	0.0028	0.0026	0.0027	0.0027	0.0027
	MMF2	0.0694	0.0110	0.0169	0.0207	0.0251	0.0100	0.0069	0.0085	0.0097	0.0141
	MMF3	0.0603	0.0275	0.0116	0.0188	0.0217	0.0169	0.0065	0.0070	0.0082	0.0475
	MMF4	0.0283	0.0237	0.0239	0.0287	0.0381	0.0023	0.0021	0.0021	0.0023	0.0025
	MMF5	0.0923	0.0789	0.0738	0.0900	0.0904	0.0027	0.0025	0.0024	0.0026	0.0028
	MMF6	0.1199	0.0693	0.0777	0.0827	0.0976	0.0025	0.0024	0.0025	0.0025	0.0025
	MMF7	0.0240	0.0209	0.0229	0.0228	0.0278	0.0024	0.0023	0.0023	0.0023	0.0025
	MMF8	0.4619	0.1197	0.1085	0.0737	0.1123	0.0026	0.0025	0.0026	0.0025	0.0026
LORD-II	MMF14	0.0490	0.0484	0.0497	0.0494	0.0502	0.0547	0.0545	0.0542	0.0548	0.0554
	MMF14_a	0.0617	0.0609	0.0613	0.0650	0.0671	0.0578	0.0563	0.0580	0.0589	0.0596
	MMF15	0.0296	0.0288	0.0291	0.0292	0.0291	0.0553	0.0551	0.0552	0.0553	0.0560
	MMF15_a	0.0374	0.0370	0.0364	0.0372	0.0378	0.0588	0.0588	0.0593	0.0594	0.0606

cases:

1. $P_{mut} = 0.00$: This case assesses the performance when only DE/rand/1/bin is used in the reproduction stage.
2. $P_{mut} = 0.25$: This case assesses the performance when DE/rand/1/bin is used more often than SBX-crossover in the reproduction stage.
3. $P_{mut} = 0.50$: This case assesses the performance when DE/rand/1/bin and SBX-crossover have equal preference and either of them is randomly selected to be used in the reproduction stage.
4. $P_{mut} = 0.75$: This case assesses the performance when SBX-crossover is used more often than DE/rand/1/bin in the reproduction stage.
5. $P_{mut} = 1.00$: This case assesses the performance when only SBX-crossover is used in the reproduction stage.

The performance of LORD with different thresholds (P_{mut}) is studied in terms of IGDX and IGDF for MMF1 to MMF8 problems. Similarly, the performance of LORD-II is studied for 3-objective MMF14, MMF14_a, MMF15 and MMF15_a problems. It should be noted that polynomial mutation [14] follows either of these reproduction strategies for perturbation of candidates so that the proposed frameworks are not prone to local optima [5]. Also, more reproduction strategies could be incorporated in Algorithm 3 of the main manuscript by growing the if-else tree.

It can be seen from Table 2 that the best performance is obtained at $P_{mut} = 0.25$. Hence, DE/rand/1/bin is preferred over SBX-crossover for exploration of search space.

Table 3: Mean of IGDX and IGDF for 2- and 3-objective MMMOPs over 51 Independent Runs.

2-objective Problems	IGDX				IGDF			
	LORD	DE-TriM [16]	MM-NAEMO [17]	MO_Ring-PSO_SCD [3]	LORD	DE-TriM [16]	MM-NAEMO [17]	MO_Ring-PSO_SCD [3]
MMF1	0.0431	0.0465 (+)	0.0486 (+)	0.0485 (+)	0.0025	0.0026 (~)	0.0040 (+)	0.0037 (+)
MMF1_a	0.0351	0.0503 (+)	0.0347 (~)	0.0352 (~)	0.0022	0.0026 (+)	0.0035 (+)	0.0036 (+)
MMF1_e	0.7499	2.8757 (+)	0.4115 (-)	0.4738 (-)	0.0029	0.0029 (~)	0.0051 (+)	0.0119 (+)
MMF2	0.0180	0.0505 (+)	0.0118 (-)	0.0416 (+)	0.0070	0.0035 (-)	0.0083 (+)	0.0207 (+)
MMF3	0.0176	0.0235 (+)	0.0137 (-)	0.0276 (+)	0.0069	0.0047 (-)	0.0085 (+)	0.0154 (+)
MMF4	0.0251	0.0211 (-)	0.0312 (+)	0.0271 (+)	0.0018	0.0025 (+)	0.0033 (+)	0.0037 (+)
MMF5	0.0814	0.0892 (+)	0.0871 (+)	0.0857 (+)	0.0024	0.0027 (+)	0.0037 (+)	0.0037 (+)
MMF6	0.0692	0.0756 (+)	0.0743 (+)	0.0736 (+)	0.0023	0.0025 (~)	0.0036 (+)	0.0035 (+)
MMF7	0.0218	0.0201 (-)	0.0229 (+)	0.0262 (+)	0.0022	0.0025 (+)	0.0035 (+)	0.0037 (+)
MMF8	0.0762	0.0989 (+)	0.3348 (+)	0.0673 (~)	0.0025	0.0029 (+)	0.0037 (+)	0.0048 (+)
MMF9	0.0046	0.0787 (+)	0.0048 (~)	0.0079 (+)	0.0085	0.0119 (+)	0.0479 (+)	0.0160 (+)
MMF10	0.0018	0.0018 (~)	0.0121 (+)	0.0276 (+)	0.0061	0.0080 (+)	0.0639 (+)	0.1128 (+)
MMF11	0.0029	0.0036 (+)	0.0418 (+)	0.0054 (+)	0.0082	0.0109 (+)	0.0931 (+)	0.0176 (+)
MMF12	0.0013	0.0013 (~)	0.0050 (+)	0.0038 (+)	0.0020	0.0021 (~)	0.0196 (+)	0.0068 (+)
MMF13	0.0242	0.0368 (+)	0.1878 (+)	0.0314 (+)	0.0063	0.0094 (+)	0.1059 (+)	0.0264 (+)
Omni-test	0.0706	0.0732 (+)	0.1511 (+)	0.3907 (+)	0.0091	0.0125 (+)	0.0130 (+)	0.0422 (+)
SYM-PART-simple	0.0549	0.0740 (+)	0.1115 (+)	0.0300 (-)	0.0165	0.0101 (-)	0.0472 (+)	0.0419 (+)
SYM-PART-rotated	0.1558	0.1885 (+)	0.7586 (+)	0.2926 (+)	0.0178	0.0125 (-)	0.0395 (+)	0.0467 (+)
Sum-up	+/-/~	14/2/2	13/3/2	14/2/2	+/-/~	10/4/4	18/0/0	18/0/0
3-objective Problems	LORD-II	DE-TriM [16]	MM-NAEMO [17]	MO_Ring-PSO_SCD [3]	LORD-II	DE-TriM [16]	MM-NAEMO [17]	MO_Ring-PSO_SCD [3]
MMF14	0.0443	0.0558 (+)	0.0465 (+)	0.0539 (+)	0.0540	0.0749 (+)	0.0808 (+)	0.0801 (+)
MMF14_a	0.0576	0.0676 (+)	0.0663 (+)	0.0613 (+)	0.0561	0.0809 (+)	0.0791 (+)	0.0789 (+)
MMF15	0.0287	0.0361 (+)	0.0518 (+)	0.0419 (+)	0.0548	0.0787 (+)	0.1113 (+)	0.0854 (+)
MMF15_a	0.0355	0.0503 (+)	0.0848 (+)	0.0452 (+)	0.0571	0.0951 (+)	0.1263 (+)	0.0841 (+)
Sum-up	+/-/~	4/0/0	4/0/0	4/0/0	+/-/~	4/0/0	4/0/0	4/0/0

This is similar to the results reported in [15] which suggests Differential Evolution (DE) generally outperforms Genetic Algorithm (GA) for multi-objective optimization problems. However, unlike the work in [15], the results reported in Table 2 suggest that a switching scheme is beneficial as it gains from the exploratory capabilities of both these reproduction strategies. It should also be noted that the IGD values (for MMF14, MMF14_a, MMF15 and MMF15_a) vary much less across different P_{mut} values from LORD-II than the IGD values for some problems (MMF2, MMF3, MMF6 and MMF8) from LORD. This suggests that LORD is more sensitive to P_{mut} than LORD-II.

4 Comparison of LORD and LORD-II with Several MAMMOEAs

In this material, three sets of comparisons are performed which are as follows:

1. As the proposed frameworks use reference vector assisted decomposition of the objective space, the performance two recent MAMMOEAs (DE-TriM [16] and MM-NAEMO [17]) using similar decomposition of objective space are compared with LORD for MMMOPs with $M = 2$ and with LORD-II for MMMOPs with

$M = 3$.

2. As LORD-II is designed for multi-modal many-objective optimization problems (MMMaOPs), its performance is compared with the only other optimizer (NIMMO [18]) developed for MMMaOPs. A few results from other competitor MMMOEAs are also presented in this comparison as these results are presented on polygon and rotated polygon problems with higher number of objectives.
3. As the recommendation of the report defining the MMMOPs [2] is followed, all the results in the main manuscript are presented with a population size of $100 \times N$ where N is the dimension of the decision space. An experiment to assess the performance of LORD-II is performed where the population size is set low, as per the optimal recommendation for MOEA/DD [8].

As the main manuscript compares LORD and LORD-II with MO_Ring_PSO_SCD [3], the first two experiments are accompanied with results from MO_Ring_PSO_SCD as well to fairly assess the relative rankings of algorithms.

4.1 Comparison with Reference Vector Assisted MMMOEAs

In this sub-section, using the parameters and reference sets specified in Section IV of the main manuscript, the performances of LORD and LORD-II are compared with Differential Evolution for Multi-Modal Multi-objective problems (DE-TriM) [16] and with the Multi-Modal Multi-objective version of Neighborhood-sensitive Archived Evolutionary Multi-Objective optimizer (MM-NAEMO) [17]. Also, the results of MO_Ring_PSO_SCD [3] are specified in Table 3 for reference. Each of these algorithms (DE-TriM, MM-NAEMO and MO_Ring_PSO_SCD) are set up using the parameters recommended in [16], [17] and [3], respectively.

Test problems from the CEC 2019 multi-modal multi-objective test suite [2] are considered for this experiment and the algorithms are run for a maximum number of $5000 \times N$ function evaluations with a $100 \times N$ population size where N is the dimension of decision space. The algorithms are executed for 51 runs and the mean of IGDX and IGDF values are reported in Table 3 to analyze the performance in decision and objective space, respectively. All the results have been statistically validated using Wilcoxon ranked sum test.

Overall, it can be seen from Table 3 that LORD-II has the best performance in both objective and decision space for 3-objective problems. LORD has the best and DE-TriM has the second-best performance in the objective space for 2-objective problems according to Table 3. On the other hand, Table 3 shows that LORD has best or second-best performance in the decision space for most of the 2-objective problems except MMF1_e. Unlike other MMMOEAs [3, 17, 19] which yields poor performance

Table 4: Mean PSP values for M -objective polygon and rotated polygon (RPolygon) problems over 31 independent runs.

M -Problems	LORD-II	NIMMO [18]	TriMOEA_TA&R [20]	MO_Ring_PSO_SCD [3]	Omni-Optimizer [21]
3-Polygon	184.66	178.71 (+)	158.39 (+)	109.85 (+)	120.17 (+)
3-RPolygon	156.01	166.54 (-)	49.63 (+)	107.81 (+)	113.59 (+)
5-Polygon	181.38	141.30 (+)	61.55 (+)	87.99 (+)	90.96 (+)
5-RPolygon	160.34	132.04 (+)	28.83 (+)	86.99 (+)	88.22 (+)
8-Polygon	216.64	111.35 (+)	72.69 (+)	69.98 (+)	71.09 (+)
8-RPolygon	196.47	104.28 (+)	13.01 (+)	67.94 (+)	70.04 (+)
10-Polygon	224.85	138.23 (+)	77.00 (+)	83.24 (+)	89.26 (+)
10-RPolygon	189.46	126.33 (+)	25.64 (+)	82.54 (+)	86.48 (+)
Sum-up	+/- / ~	7/1/0	8/0/0	8/0/0	8/0/0

Table 5: Mean IGDX values for M -objective polygon and rotated polygon (RPolygon) problems over 31 independent runs.

M -Problems	LORD-II	NIMMO [18]	TriMOEA_TA&R [20]	MO_Ring_PSO_SCD [3]	Omni-Optimizer [21]
3-Polygon	0.0054	0.0056 (+)	0.0063 (+)	0.0091 (+)	0.0083 (+)
3-RPolygon	0.0064	0.0059 (-)	0.0295 (+)	0.0090 (+)	0.0085 (+)
5-Polygon	0.0055	0.0070 (+)	0.0162 (+)	0.0113 (+)	0.0110 (+)
5-RPolygon	0.0062	0.0074 (+)	0.0400 (+)	0.0113 (+)	0.0110 (+)
8-Polygon	0.0046	0.0089 (+)	0.0136 (+)	0.0143 (+)	0.0140 (+)
8-RPolygon	0.0051	0.0093 (+)	0.0747 (+)	0.0144 (+)	0.0138 (+)
10-Polygon	0.0044	0.0072 (+)	0.0123 (+)	0.0120 (+)	0.0112 (+)
10-RPolygon	0.0053	0.0076 (+)	0.0404 (+)	0.0118 (+)	0.0112 (+)
Sum-up	+/- / ~	7/1/0	8/0/0	8/0/0	8/0/0

in objective space in order to improve the performance in decision space, LORD and LORD-II performs satisfactorily in both the spaces and competitively outperforms the other reference vector assisted algorithms for MMMOEAs.

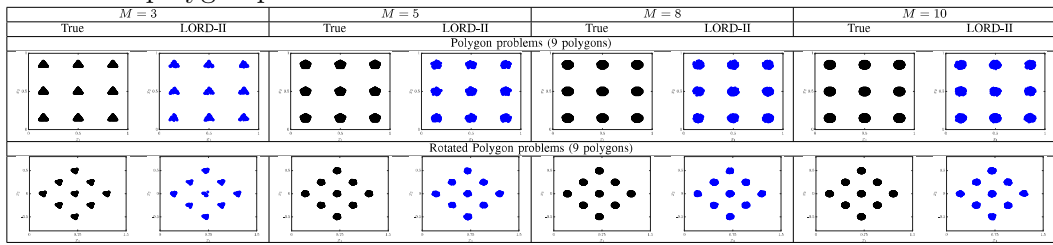
4.2 Comparison on Multi-Modal Many-Objective Problems

In this sub-section, the performance of LORD-II is compared with Niching Indicator based Multi-Modal Many-Objective optimizer (NIMMO) [18] which is set up as per the specifications in [18]. Also, the performance of MO_Ring_PSO_SCD [3] on these problems are specified for reference, along with that of the first MMMOEA (Omni-Optimizer [21]) and the scalable MMMOEA (TriMOEA_TA&R [20]).

Table 6: Mean IGDF values for M -objective polygon and rotated polygon (RPolygon) problems over 31 independent runs.

M -Problems	LORD-II	NIMMO [18]	TriMOEA _TA&R [20]	MO_Ring_ PSO_SCD [3]	Omnio- Optimizer [21]
3-Polygon	0.0023	0.0025 (+)	0.0040 (+)	0.0034 (+)	0.0028 (+)
3-RPolygon	0.0023	0.0025 (+)	0.0046 (+)	0.0034 (+)	0.0028 (+)
5-Polygon	0.0031	0.0044 (+)	0.0149 (+)	0.0057 (+)	0.0051 (+)
5-RPolygon	0.0030	0.0044 (+)	0.0149 (+)	0.0058 (+)	0.0052 (+)
8-Polygon	0.0031	0.0069 (+)	0.0180 (+)	0.0092 (+)	0.0082 (+)
8-RPolygon	0.0032	0.0069 (+)	0.0190 (+)	0.0093 (+)	0.0083 (+)
10-Polygon	0.0033	0.0064 (+)	0.0204 (+)	0.0087 (+)	0.0074 (+)
10-RPolygon	0.0034	0.0064 (+)	0.0185 (+)	0.0086 (+)	0.0075 (+)
Sum-up	+ / - / ~	8/0/0	8/0/0	8/0/0	8/0/0

Table 7: Cartesian coordinate plots of the 2-dimensional PSs of M -objective polygon and rotated polygon problems.



This experiment considers M -objective polygon and rotated (by 45 degrees) polygon problems [18, 22]. For these problems, the number of objectives (M) is equal to the number of vertices of the polygons and i^{th} objective to be minimized is given by the Euclidean distance of a solution to its nearest i^{th} vertex over any of the given number of polygons. Hence, a 3-objective polygon problem searches for triangles, a 5-objective polygon problem searches for pentagons and so on. There are a total of eight problem instances considered in this experiment. These problems are specified as follows:

- Dimension of decision space: $N = 2$
- Bounds of decision space (\mathcal{D}): $\mathbf{X}^L = [-1, -1]$ and $\mathbf{X}^U = [2, 2]$
- Dimension of objective space: $M \in \{3, 5, 8, 10\}$
- Number of Subsets in Pareto-optimal Set: #Sets = number of polygons = 9

Table 8: Specifications for the experiment on polygon and rotated polygon problems according to [18].

Parameters		Used by LORD-II	Used by NIMMO, TriMOEA_TA&R, MO_Ring_PSO_SCD, and Omni-Optimizer in [18]
n_{pop}	3-obj	210	210
	5-obj	210	210
	8-obj	156	156
	10-obj	230	230
#runs		31	31
MaxFES		10000	10000
N_{IGD}		5000	5000

- Reference sets for true PS and true PF as well as the vertices of the polygons are obtained from <https://sites.google.com/view/nimmopt/>.

As per the recommendations in [18], this experiment considers the specifications mentioned in Table 8. Here, PSP, IGDX and IGDF values are reported in Tables 4, 5 and 6, respectively. Apart from LORD-II, all the performance values are considered from the results in [18] as all the recommendations of [18] are used to conduct this experiment with polygon and rotated polygon problems. The remaining parameters of LORD-II are set up as specified in Section IV of the main manuscript.

Results demonstrate the superiority of LORD-II in both the decision and objective spaces, over all the problems, among the five state-of-the-art competitor algorithms considered in this experiment. An interesting observation is that the performance of all MMMOEAs (except TriMOEA_TA&R) in both decision and objective spaces are unaffected due to rotation. However, the IGDX and PSP values of TriMOEA_TA&R are widely different (poorer) for rotated polygon problems from that of the polygon problems (Tables 4 and 5, respectively). This may be due to the ignorance of solution distribution in the decision space by TriMOEA_TA&R and solely focusing on the number of solutions per PS as the diversity criteria in the decision space [20].

The distribution of the solutions as obtained by the median run of LORD-II over the 9 subsets in the PS of the 8 instances of the test problems are presented in Table 7 which are then compared with the ground truth for analysis. The following observations are noted:

- For all the 8 instances, LORD-II converges to global surfaces i.e., there are no outliers.
- For most of the cases, the number of solutions per subset is uniform over the 9

Table 9: Mean of IGDX and IGDF for M -objective MMMOPs over 51 Independent Runs for Different Population Sizes (n_{pop}).

Problems	M	Recommended Population Size for MOEA/DD in [8]				Recommended Population Size for MMMOPs in [2]			
		IGDX		IGDF		IGDX		IGDF	
		n_{pop}	LORD-II	MOEA/DD	LORD-II	MOEA/DD	n_{pop}	LORD-II	MOEA/DD
MMF14	3	91	0.0832	0.2150 (+)	0.1044	0.1045 (~)	300	0.0443	0.0671 (+)
MMF14_a	3	91	0.1150	0.2076 (+)	0.1044	0.1045 (~)	300	0.0576	0.0780 (+)
MMF15	3	91	0.0514	0.0522 (~)	0.1055	0.1056 (~)	300	0.0287	0.0295 (+)
MMF15_a	3	91	0.0638	0.0705 (+)	0.1056	0.1144 (+)	300	0.0355	0.0357 (~)
MMF14	5	210	0.3070	0.3314 (+)	0.3125	0.3136 (+)	495	0.2448	0.2554 (+)
MMF14_a	5	210	0.3283	0.4083 (+)	0.3129	0.3135 (~)	495	0.2670	0.2846 (+)
MMF15	5	210	0.2460	0.2652 (+)	0.3155	0.3167 (+)	495	0.1960	0.2032 (+)
MMF15_a	5	210	0.2695	0.2963 (+)	0.3181	0.3168 (-)	495	0.2155	0.2230 (+)
MMF14	8	156	0.6864	0.7006 (+)	0.7233	0.7244 (+)	828	0.5621	0.5857 (+)
MMF14_a	8	156	0.6851	0.7363 (+)	0.7225	0.7241 (+)	828	0.5725	0.5936 (+)
MMF15	8	156	0.6086	0.6263 (+)	0.7270	0.7291 (+)	828	0.5146	0.5586 (+)
MMF15_a	8	156	0.6543	0.6539 (~)	0.7277	0.7289 (+)	828	0.5315	0.5498 (+)
Sum-up			+/-/~	14/0/2	+/-/~	11/1/4	+/-/~	15/0/1	+/-/~
									10/2/4

subsets in the PS.

- It can be seen that for both polygon and rotated polygon problems, the shape and size of the polygon are properly replicated for 3- and 5-objective problems. For 8- and 10-objective problem, the shapes are not identifiable, rather a near-spherical blob is formed at each of the subset in the PS.

4.3 Comparing recommended population size of MOEA/DD

The experiments in the main manuscript with respect to LORD-II for MMMOPs with $M \geq 3$ are provided with a population size of approximately $100 \times N$ (as recommended by the paper proposing the MMMOPs [2]) where N is the number of decision variables. On one hand, such large population size is a necessity for MMMOPs (please see Section I of main manuscript), on the other hand, it is questionable whether MOEAs such as MOEA/DD works well with such large population size. This further raises the question of whether the superior performance of LORD-II over MOEA/DD in Table V of the main manuscript is an attribute of the proposed algorithm or is only a result of the large population size.

For fair comparison, this experiment is proposed where both LORD-II and MOEA/DD are executed using the small population size recommended in the paper proposing MOEA/DD [8]. The IGDX and IGDF values for both the algorithms executed using large and small population sizes are reported in Table 9. The following insights are obtained from Table 9:

- As can be seen, the improved performance of LORD-II with respect to MOEA/DD is once again evident even for small population size.
- For none of the test instances, LORD-II is outperformed by MOEA/DD in the decision space. Only in one test instance for small population size and two test instances for large population size, MOEA/DD outperforms LORD-II in the objective space. However, the numerical values are different only by a small margin.
- As population size affects IGDX and IGDF, a large population size reflects better results regardless of the effectiveness of the underlying EA [18]. This better performance for larger population size is also observed in Table 9 for both LORD-II and MOEA/DD. However, as the superior performance of LORD-II is also established for small population size, this better result of LORD-II against MOEA/DD is indeed due to the effectiveness of the proposed algorithmic framework of LORD-II.

Thus, it is clearly established that the improved performance is an attribute of the proposed algorithmic framework (LORD-II) and not of the large population size.

5 Comparison by Visualization of Results

The Cartesian coordinate plots of the 2-objective MMMOPs are presented in Tables 10 and 11. For comparison, the results of LORD, MO_Ring_PSO_SCD [3] and the ground truth (ideal solutions) are plotted. Similarly, the Cartesian coordinate plots of the 3-objective MMMOPs are presented in Table 12 for comparing the results of LORD-II, MO_Ring_PSO_SCD [3] and the ground truth (ideal solutions).

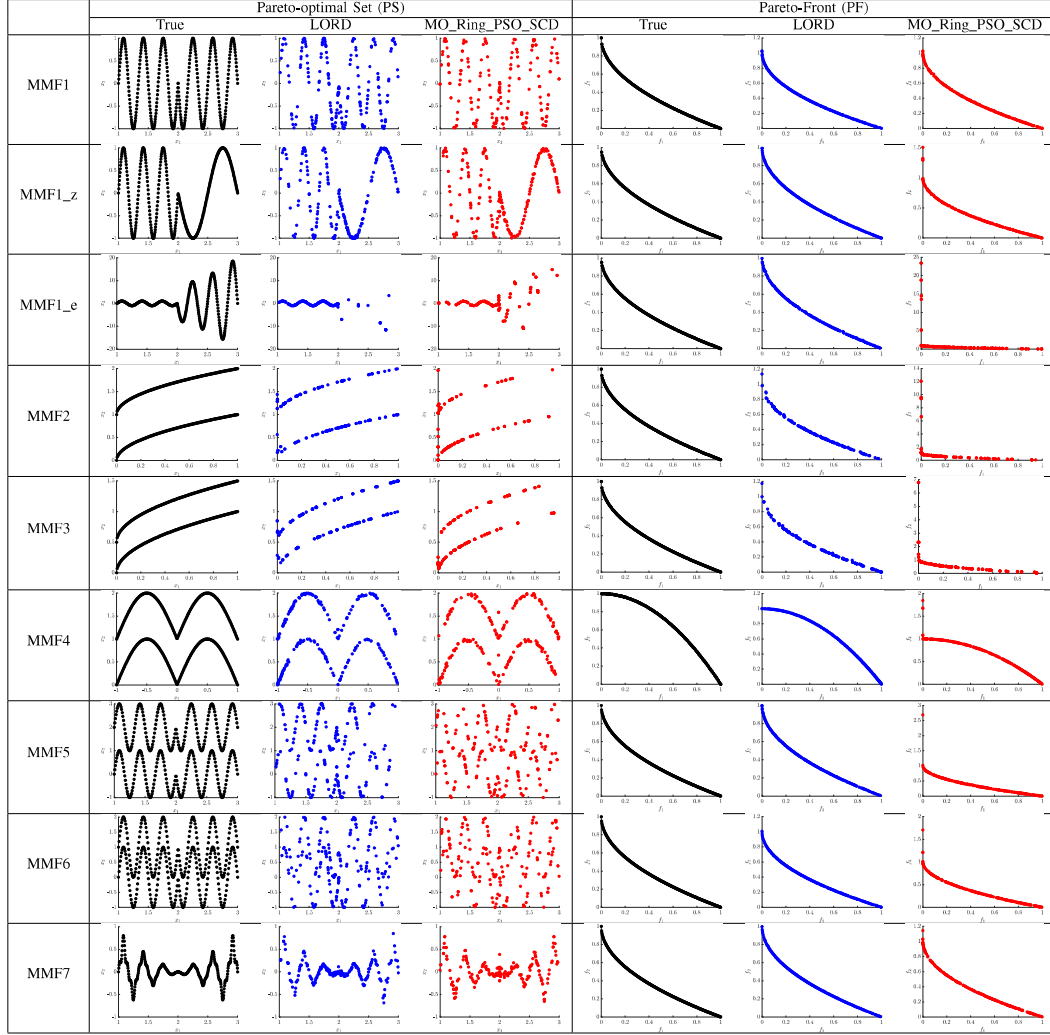
5.1 Performance of LORD in objective space

It can be seen from Tables 10 and 11 that in most of the cases the number of outliers (points which have not converged on the ideal surface of PF) present in the results of MO_Ring_PSO_SCD are much more than those of LORD. This indicates the better convergence of LORD than MO_Ring_PSO_SCD. However, just on the basis of the plots, it is difficult to conclude regarding the diversity of solutions in the objective space as both the algorithms produce relatively uniform solution distribution.

5.2 Performance of LORD in decision space

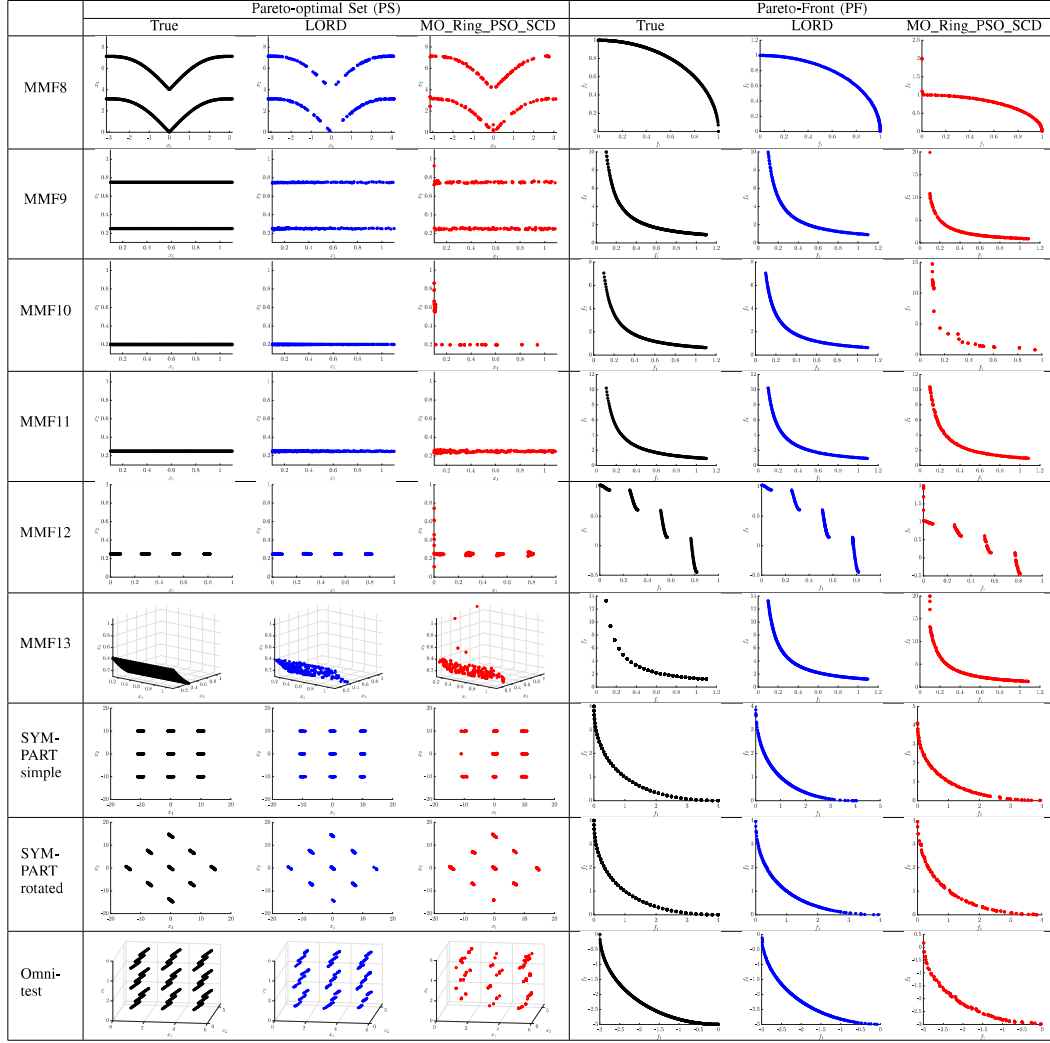
From Tables 10 and 11, it can be seen for all MMMOPs except MMF1_e and MMF8, the solution distribution in the decision space is atleast as good as that provided by

Table 10: Cartesian coordinate plots of PSs and PFs for some 2-objective MMMOPs viz. MMF1 to MMF7 and MMF1_z and MMF1_e.



MO_Ring_PSO_SCD. In some cases, such as MMF2, MMF3 and MMF10, the solution distribution is evidently superior than those obtained by MO_Ring_PSO_SCD. The poor performance for MMF1_e and MMF8 indicates the need for better decomposition methods in the decision space.

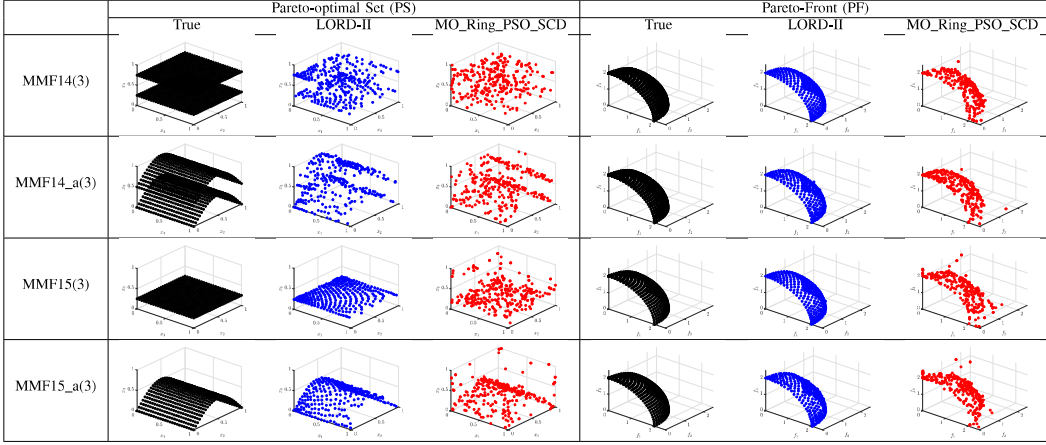
Table 11: Cartesian coordinate plots of PSs and PFs for some 2-objective MMMOPs viz. MMF8 to MMF13 and Omni-test, SYM-PART simple and SYM-PART rotated.



5.3 Performance of LORD-II in objective space

While MMF14 and MMF14_a are implemented to have one global PF, MMF15 and MMF15_a have one global and one local PF. The PFs for these problems are a spherical non-convex surface with the global being located at a radius of 2 and the local being located at a radius of 2.2, centering the origin of the objective space, in the first hyper-octant. As seen from Table 12, in the same function evaluation budget,

Table 12: Cartesian coordinate plots of PSs and PFs for 3-objective MMMOPs.



almost all candidates have converged on the global surface of PF for LORD-II which is not the case for MO_Ring_PSO_SCD.

5.4 Performance of LORD-II in decision space

To realize the reason behind presence of outliers for MO_Ring_PSO_SCD, the corresponding decision space can be analyzed. While MMF14 and MMF14_a are implemented to have two global PSs, MMF15 and MMF15_a has one global and one local PS. As shown in the true solutions in Table 12, the top-most PS for MMF14 and MMF14_a acts as a local PS for MMF15 and MMF15_a, respectively.

By looking into the decision space, it can be realized that for MMF15 and MMF15_a, many solutions are stuck at the local optimal surface for MO_Ring_PSO_SCD which has been successfully overcome by LORD-II. This establishes the superiority of LORD-II over MO_Ring_PSO_SCD.

6 Scalability Study on LORD-II framework

As argued in [20], most of the MAMMOEAs in literature are not tested on scalable problems which raises doubts about the scalability of the MAMMOEAs. In this section, the performance of LORD-II is analyzed by varying the candidate dimension (N) of 3-objective MMF14 problem i.e., for $N = \{3, 10, 30, 50, 100\}$. The other parameters are kept same those mentioned in the main manuscript for 3-objective MMF14 problem. The mean of 51 runs (odd number of runs to get distinct median runs for each metric) are noted in Table 13.

Table 13: Mean of rPSP, IGDX, rHV and IGDF for 3-objective MMF14 (with different candidate dimensions, N) over 51 Independent Runs of LORD-II.

N	rPSP	IGDX	rHV	IGDF
3	0.0449	0.0443	1.0395	0.0540
10	0.5928	0.5838	1.0414	0.0013
30	2.8270	1.5038	1.0402	0.0001
50	2.1513	2.1258	1.0405	0.0001
100	3.2476	3.1807	1.0406	0.0000

As the number of objectives (M) does not change, the performance in the objective space is expected to remain almost same. This is true for rHV. However, it is interesting to note that IGDF gradually decreases i.e., the performance of LORD-II improves with increase in N .

At first, the performance in the decision space deteriorates only linearly (not exponentially) with increase in N . For example, IGDX increases 34 times when N is increased from 3 to 30. However, with further increase in N , the deterioration in performance is very less. For example, IGDX increases by only twice when N is increased from 30 to 100.

Based on this experiment, it is claimed the performance of LORD-II with the proposed approaches for decomposition of decision and objective spaces work efficiently even for high dimensional MMMOPs i.e., the proposed frameworks are scalable with problem size.

7 Population Dynamics in Decision and Objective Space

The experiment performed in [3], which studies and compares the convergence behavior of MO_Ring_PSO_SCD in the decision space, is repeated in this work for comparing the corresponding behavior of LORD and LORD-II with MO_Ring_PSO_SCD [3] and DN-NSGA-II [23]. For this experiment, the proportion of solutions in each of the four distinct regions of MMF4 (Fig. 1a) is calculated per generation. Ideally, for uniformly distributed solutions, these proportions should reach and saturate at 25%. For all the EAs, $n_{pop} = 800$ and $G_{max} = 100$ is considered with the remaining parameters as specified in Section IV of the main manuscript. Each of the EAs are allowed to run 5 times and the mean proportions are plotted for DN-NSGA-II (Fig. 1b), MO_Ring_PSO_SCD (Fig. 1c), LORD (Fig. 1d) and LORD-II (Fig. 1e). As seen from these figures, the proportion of solutions in 3 regions is steady near 25-27% for

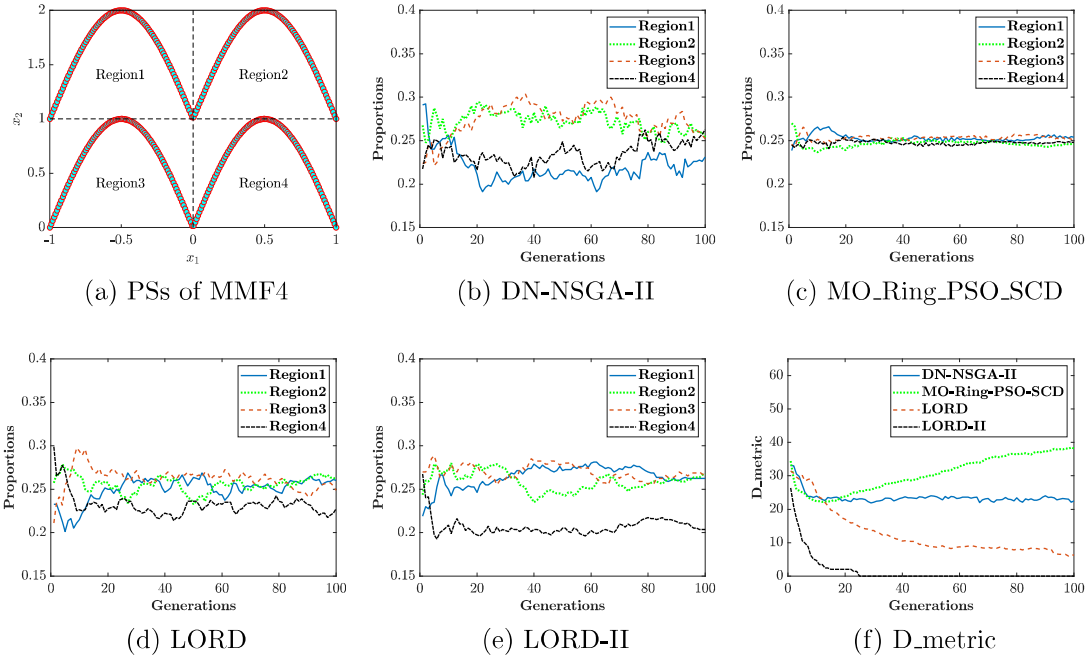


Figure 1: Solution distribution of MMF4 problem in the decision space (a), population dynamics in the decision space for four algorithms: DN-NSGA-II (b), MO_Ring_PSO_SCD (c), LORD (d) and LORD-II (e), population dynamics in the objective space using D_metric for these algorithms (f).

both LORD and LORD-II. For LORD, the proportion in region 4 fluctuates between 20 to 25%, whereas for LORD-II, it is steady around 19-21%. Thus, the convergence behavior of LORD and LORD-II is intermediate between that of MO_Ring_PSO_SCD and DN-NSGA-II.

Along with the diversity of solution in decision space, the diversity of solution in objective space is also important. For this experiment, D_metric [10] is used as given by (5) with $n_{dir} = 800$. D_metric indicates the deviation between ideal and actual solution distribution in the objective space at the G^{th} generation and hence, it should be 0 ideally.

For the population at each generation, D_metric is obtained for all the four EAs and plotted in Fig. 1f. As shown, the diversity of solutions in objective space for MO_Ring_PSO_SCD severely deteriorates with generations. This may be a result of the crowding illusion described in Fig. 2 of the main manuscript. On the other hand, for LORD, although D_metric has not reached 0, a decreasing trend is observed. For LORD-II, the D_metric has reached the ideal value roughly by 25 generations. These

evidences support the enhanced diversity preservation of the proposed frameworks in the objective space without sacrificing too much on the distribution in the decision space.

All the above-mentioned experiments establish the efficacy and the robustness of using the proposed LORD and LORD-II frameworks for addressing multi-objective optimization problems (MMMOPs or otherwise).

8 Conclusion

As the modality of a real-world problem is often unknown, an evolutionary algorithm designed for MMMOPs, should also perform equally good for unimodal multi-objective optimization problems. Moreover, the convergence in the objective space is the foremost criteria to be established before dealing with the solution distributions in the objective and decision space. The proposed frameworks, LORD and LORD-II, provide themselves as robust alternatives for various kinds of multi-objective and many-objective optimization problems, respectively. Nonetheless, it is a preliminary work in this direction and better methods for improving the performance of evolutionary algorithms for MMMOPs are open for further research.

References

- [1] Ryoji Tanabe and Hisao Ishibuchi. A review of evolutionary multi-modal multi-objective optimization. *IEEE Transactions on Evolutionary Computation*, pages 1–9, 2019.
- [2] J. J. Liang, B. Y. Qu, D. W. Gong, and C. T. Yue. Problem definitions and evaluation criteria for the CEC special session on multimodal multiobjective optimization. *Technical Report, Computational Intelligence Laboratory, Zhengzhou University*, 2019.
- [3] Caitong Yue, Boyang Qu, and Jing Liang. A multiobjective particle swarm optimizer using ring topology for solving multimodal multiobjective problems. *IEEE Transactions on Evolutionary Computation*, 22(5):805–817, Oct 2018.
- [4] S. Bandyopadhyay and A. Mukherjee. An algorithm for many-objective optimization with reduced objective computations: A study in differential evolution. *IEEE Transactions on Evolutionary Computation*, 19(3):400–413, 2015.

- [5] K. Deb, A. Pratap, S. Agarwal, and T. Meyarivan. A fast and elitist multiobjective genetic algorithm: NSGA-II. *IEEE Transactions on Evolutionary Computation*, 6(2):182–197, 2002.
- [6] Ye Tian, Xingyi Zhang, Ran Cheng, and Yaochu Jin. A multi-objective evolutionary algorithm based on an enhanced inverted generational distance metric. In *2016 IEEE Congress on Evolutionary Computation (CEC)*, pages 5222–5229, July 2016.
- [7] P. A. N. Bosman and D. Thierens. The balance between proximity and diversity in multiobjective evolutionary algorithms. *IEEE Transactions on Evolutionary Computation*, 7(2):174–188, 2003.
- [8] Ke Li, Kalyanmoy Deb, Qingfu Zhang, and Sam Kwong. An evolutionary many-objective optimization algorithm based on dominance and decomposition. *IEEE Transactions on Evolutionary Computation*, 19(5):694–716, 2015.
- [9] J. Bader and E. Zitzler. HypE: An algorithm for fast hypervolume-based many-objective optimization. *Evolutionary computation*, 19(1):45–76, 2011.
- [10] Raunak Sengupta, Monalisa Pal, Sriparna Saha, and Sanghamitra Bandyopadhyay. Population dynamics indicators for evolutionary many-objective optimization. In Chhabi Rani Panigrahi, Arun K. Pujari, Sudip Misra, Bibudhendu Pati, and Kuan-Ching Li, editors, *Progress in Advanced Computing and Intelligent Engineering*, pages 261–271 (in Press), Singapore, 2019. Springer Singapore.
- [11] Ye Tian, Ran Cheng, Xingyi Zhang, Fan Cheng, and Yaochu Jin. An indicator based multi-objective evolutionary algorithm with reference point adaptation for better versatility. *IEEE Transactions on Evolutionary Computation*, 2017.
- [12] Xianpeng Wang, Zhiming Dong, and Lixin Tang. Multiobjective differential evolution with personal archive and biased self-adaptive mutation selection. *IEEE Transactions on Systems, Man, and Cybernetics: Systems*, pages 1–13, 2018.
- [13] Kalyanmoy Deb and Himanshu Jain. An evolutionary many-objective optimization algorithm using reference-point-based nondominated sorting approach, part I: Solving problems with box constraints. *IEEE Transactions on Evolutionary Computation*, 18(4):577–601, 2014.
- [14] Li-Min Li, Kang-Di Lu, Guo-Qiang Zeng, Lie Wu, and Min-Rong Chen. A novel real-coded population-based extremal optimization algorithm with polynomial mutation: A non-parametric statistical study on continuous optimization problems. *Neurocomputing*, 174:577 – 587, 2016.

- [15] Tea Tušar and Bogdan Filipič. Differential evolution versus genetic algorithms in multiobjective optimization. In Shigeru Obayashi, Kalyanmoy Deb, Carlo Poloni, Tomoyuki Hiroyasu, and Tadahiko Murata, editors, *Evolutionary Multi-Criterion Optimization*, pages 257–271, Berlin, Heidelberg, 2007. Springer Berlin Heidelberg.
- [16] Monalisa Pal and Sanghamitra Bandyopadhyay. Differential evolution for multimodal multi-objective problems. In *Proceedings of the Genetic and Evolutionary Computation Conference Companion*, GECCO ’19, pages 1399–1406, New York, NY, USA, 2019. ACM.
- [17] K. Maity, R. Sengupta, and S. Saha. MM-NAEMO : Multimodal neighborhood-sensitive archived evolutionary many-objective optimization algorithm. In *2019 IEEE Congress on Evolutionary Computation (CEC)*, pages 286–294, June 2019.
- [18] Ryoji Tanabe and Hisao Ishibuchi. A niching indicator-based multi-modal many-objective optimizer. *Swarm and Evolutionary Computation*, 49:134 – 146, 2019.
- [19] Qin Qin Fan and Xuefeng Yan. Solving multimodal multiobjective problems through zoning search. *IEEE Transactions on Systems, Man, and Cybernetics: Systems*, pages 1–12, 2019.
- [20] Yiping Liu, Gary G. Yen, and Dunwei Gong. A multi-modal multi-objective evolutionary algorithm using two-archive and recombination strategies. *IEEE Transactions on Evolutionary Computation*, 23(4):660–674, Aug 2019.
- [21] Kalyanmoy Deb and Santosh Tiwari. Omni-optimizer: A procedure for single and multi-objective optimization. In Carlos A. Coello Coello, Arturo Hernández Aguirre, and Eckart Zitzler, editors, *Evolutionary Multi-Criterion Optimization*, pages 47–61, Berlin, Heidelberg, 2005. Springer Berlin Heidelberg.
- [22] Hisao Ishibuchi, Naoya Akedo, and Yusuke Nojima. A many-objective test problem for visually examining diversity maintenance behavior in a decision space. In *Proceedings of the 13th Annual Conference on Genetic and Evolutionary Computation*, GECCO ’11, pages 649–656, New York, NY, USA, 2011. ACM.
- [23] J. J. Liang, C. T. Yue, and B. Y. Qu. Multimodal multi-objective optimization: A preliminary study. In *2016 IEEE Congress on Evolutionary Computation (CEC)*, pages 2454–2461. IEEE, 2016.